Supporting Information

Phenazine-based non-fused electron acceptors for high performance organic solar cells

Tingting Wang, Wenliang Li, Jie Xu, Chaokang Hu, Wenli Luo, Xiaohong Zhao,* Yu Hu and Zhongyi Yuan

T. Wang, W. Li, J. Xu, C. Hu, W. Luo, X. Zhao, Y. Hu, Prof. Z. Yuan

College of Chemistry and Chemical Engineering/ Film Energy Chemistry for Jiangxi Provincial Key Laboratory (FEC)

Nanchang University

999 Xuefu Avenue, Nanchang 330031, China.

E-mail: zhaoxh@ncu.edu.cn

Contents

1. Experimental Section

1.1 Material Measurements

The ^{1}H NMR and ^{13}C NMR spectra of all the synthesized materials were taken with $CDCl_3$ as the solution, and measured on 400 MHz nuclear magnetic resonance (NMR) spectrometer. UV-vis absorption spectra were recorded on a PerkinElmer Lambda 750 Spectrophotometer. Fluorescence spectra were measured by photoluminescence spectroscopy (Hitachi F- 7000). Energy level measurements were performed using electrochemical cyclic voltammetry (CV), and the energy level was calculated using the equation：

$$E_{LUMO} = -e(\varphi_{red} + 4.80)\ (eV) \text{ and } E_{HOMO} = -e(\varphi_{ox} + 4.80)\ (eV)$$

The tests were performed separately using the glassy carbon, Ag/AgCl and Pt wire as Working electrode, reference electrode and auxiliary electrode; electrolyte: tetrabutylammonium hexafluoro-phosphate (Bu_4NPF_6); internal standard: ferrocene (Fc).The ground state geometry of molecular was optimized by using the Density Functional Theory (DFT) method at a B3LYP/6-31 G (d, p) level. All the calculations of the acceptor molecules were performed using the Gaussian 09 package.[1]

1.2 Device Fabrication and Characterization

Conventional bulk phase heterojunction solar cells devices with ITO/PEDOT:PSS/active layers/PDINO/Ag structures were used. In fabricating the OSCs devices, the conductive ITO substrates were ultrasonically cleaned with detergent, water, acetone, and isopropanol in that order. After drying the ITO substrate and treating the surface with UV ozone for 20 minutes, PEDOT:PSS solution filtered with a 0.45 μm PES filter was then spin-coated on the ITO surface at 4000 rpm for 30 s. After thermal annealing at 150 ℃ for 18 minutes, the substrates were transferred to

a nitrogen-filled glove box. The active layer was then spin-coated with a donor:acceptor (1:1.2 w/w) solution in $CHCl_3$ at a total concentration of 14.3 mg mL^{-1} at 3000 rpm with a final layer thickness of about 100 nm. The active layer was thermally annealed at 100 ℃ for 10 minutes, and then, a cathodic interfacial layer PDINO of 3 mg mL^{-1} was spin-coated on the top surface of the active layer at 3000 rpm for 30 s. Ag (80 nm) was deposited by thermal evaporation under a vacuum chamber to complete the device fabrication. The effective area of one cell was 0.04 cm^2.

The current-voltage (*J–V*) characteristics were measured by a Keithley 2400 Source Meter under simulated solar light (100 mW cm^{-2}, AM 1.5 G, Abet Solar Simulator Sun 2000). The incident photon-to-electron conversion efficiency (IPCE) spectra were detected on an IPCE measuring system (Oriel Cornerstone monochromator equipped with Oriel 70613NS QTH lamp). All the measurement was performed at room temperature under nitrogen atmosphere. The external quantum efficiency (EQE) data were recorded with a QE-R3011 test system from Enli technology company (Taiwan).

The photocurrent (J_{ph}) versus light intensity (P_{light}) was used to quantify the charge recombination dynamics. The correlation between J_{sc} and P_{light} was expressed as a power-law equation of $J_{sc} \propto P_{light}^{\alpha}$. If all free charge carriers are swept out and collected at the electrodes prior to recombination, α is supposed to be 1, while $\alpha < 1$, bimolecular recombination exists.[2]

1.3 Mobility measurements

electron-only devices (ITO/ZnO/active layers/PDINO/Ag.) and Hole-only devices (ITO/PEDOT:PSS/active layers/MoO_3/Ag) were fabricated to evaluate the electron and hole mobilities (μ_e and μ_h) of blend films by the space-charge limited current (SCLC) model.The mobilities were determined by fitting the dark current based on a single-carrier SCLC model, which is described by the following equation:

$$J = 9\varepsilon_0\varepsilon_r\mu V^2/8L^3$$

Where *J* is the current density, ε_0 is the permittivity of free space (8.85×10^{-12} F m^{-1}), ε_r

is the relative dielectric constant of transport medium, μ is the internal voltage in the device, V is the internal voltage in the device, L is the film thickness of the active layer, ($L \approx 100$ nm), which was measured by step profiler.

1.4 AFM and Contact-angle measurements

The film morphology was measured by atomic force microscopy (AFM) with the tapping mode from Asylum Research.[3] And the film for AFM measurements was prepared using the same procedures as OSCs device, without Ag and cathodic interface layer.

Deionized water and diiodomethane were used as calibration liquids, respectively, and contact angle measurements of neat films were employed to estimate the surface free energy (SFE) of the films. The surface energy γ values could be calculated according to the Wu model on the neat films by the Equation:

$$\gamma = \gamma^{d} + \gamma^{p}$$

$$\gamma_{LV}(1+\cos\theta) = 4\,\gamma_S{}^{d}\gamma_L{}^{d} / (\gamma_S{}^{d}+\gamma_L{}^{d}) + 4\,\gamma_S{}^{P}\gamma_L{}^{P} / (\gamma_S{}^{P}+\gamma_L{}^{P})$$

the γ is the sum of dispersion (d) and polar (p) components. The interfacial tension between two different materials can be calculated by the following equation:

$$\gamma_{D:A} = \gamma_D + \gamma_A - 2\sqrt{\gamma_D\gamma_A}e^{[-\beta(\gamma_D-\gamma_A)^2]}$$

$\gamma_{D:A}$represents the surface energy of the interface between D and A, β= 0.000115 m^4 mJ^{-2}.[4]

2. Synthesis Section

2.1 Structure of Existing excellent NFREAs

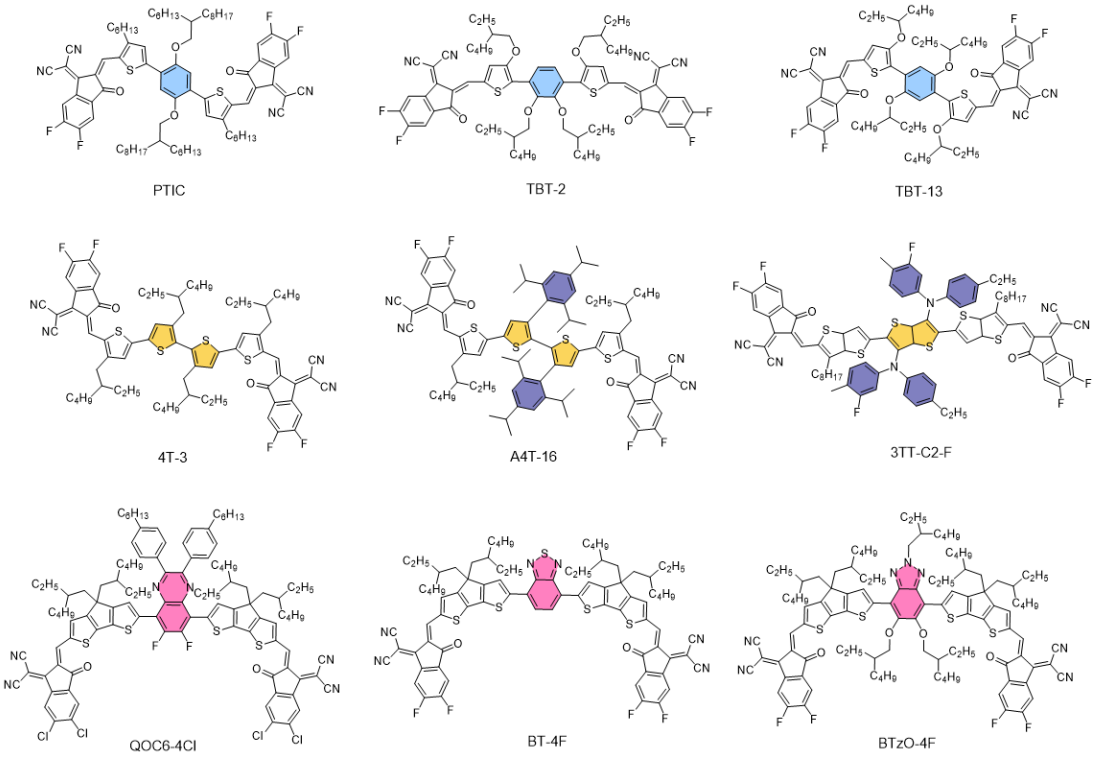

Fig. S1 Structure of existing excellent NFREAs.[5-11]

2.2 Materials

All solvents and reagents used were purchased from commercial sources without further purification and compounds 1a and 1b were synthesized with reference to literature methods.[12] Column chromatography was carried out on silica gel (100-200 mesh). 2-(5,6-difluoro-3-oxo-2,3-dihydro-1H-inden-1-ylidene)malononitrile and 2-(5,6-dichloro-3-oxo-2,3-dihydro-1H-inden-1-ylidene)malononitrile Purchase from Pulsar Chemical.

2.3 Synthetic details of FQ-4F, FQ-FCl, and FQ-4Cl

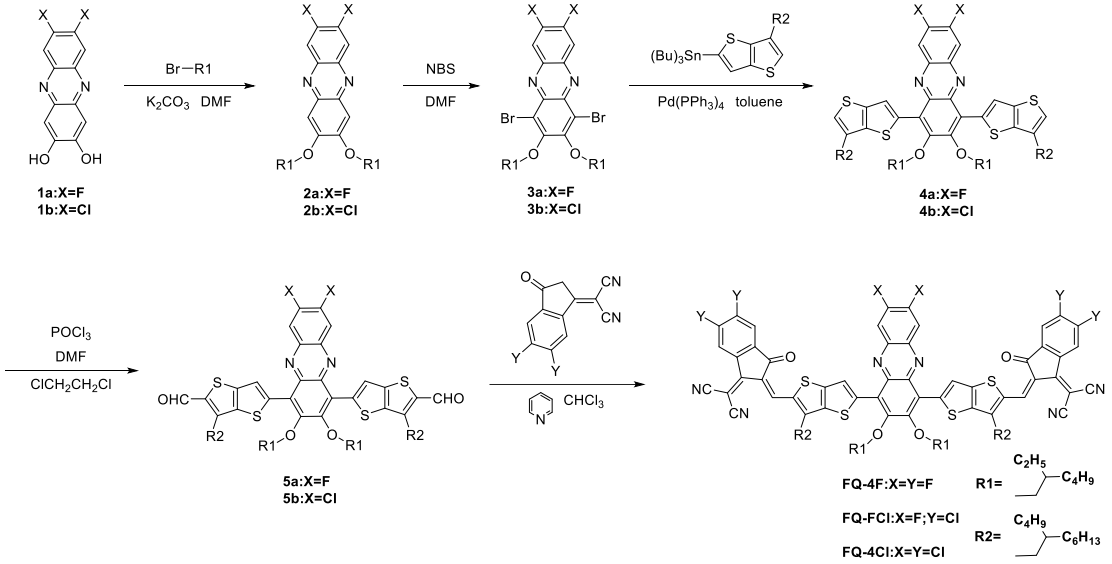

Scheme S1. Synthetic routes of FQ-4F、FQ-FCl、FQ-4Cl

FQ-4F、FQ-FCl、FQ-4Clwere obtained following the synthetic routes as shown in Scheme 1.

2,3-bis((2-ethylhexyl)oxy)-7,8-difluorophenazine(compound 2a)： Compound 1a (2 g, 8.06 mmol) was dissolved in 30 mL *N*,*N*-Dimethylformamide (DMF) followed by the addition of K_2CO_3 (3.34 g, 24.18 mmol), 1-bromo-2-ethylhexane (3.89 g, 20.15 mmol) was then added to the mixture and stirred at 85 °C for 12 h. After cooling the reactant to room temperature, the product was poured into water (200 mL) and extracted by dichloromethane (DCM, 3*50 mL). Subsequently, the mixture was washed twice with water (100 mL) and compound 2a was purified by silica gel column chromatography with PE/DCM = (2:1, v/v) as eluent with a yield of 86%.

Compound2a： ^{1}HNMR(400 MHz, Chloroform-d) δ 7.81 (t, J = 9.5 Hz, 2H), 7.27 (s, 2H), 4.07 (d, J = 5.7 Hz, 4H), 1.90 – 1.83 (m, 2H), 1.52 (dq, J = 22.6, 7.5 Hz, 9H), 1.29 (d, J = 42.9 Hz, 12H), 0.94 (dd, J = 24.7, 7.5 Hz, 14H). ^{13}C NMR (101 MHz, Chloroform-d) δ 155.12, 153.46, 153.28, 150.90, 150.71, 141.91, 138.83, 138.78, 113.59, 113.52, 113.46, 113.40, 104.94, 71.62, 71.60, 39.20, 30.64, 30.63, 29.66, 29.06, 24.02, 24.00, 23.00, 14.01, 11.17.

Compound2b： ^{1}H NMR (400 MHz, Chloroform-*d*) δ 8.18 (s, 2H), 7.23 (s, 2H), 4.08 (d, *J* = 5.6 Hz, 4H), 1.86 (s, 2H), 1.52 (dq, *J* = 22.5, 7.4 Hz, 12H), 1.35 (s, 12H),

0.97 – 0.90 (m, 12H).^{13}C NMR (101 MHz, Chloroform-d) δ 155.57, 142.60, 140.15, 132.95, 129.07, 105.00, 71.67, 71.65, 39.20, 30.64, 30.62, 29.06, 24.02, 24.00, 23.01, 14.02, 11.19.

1,4-dibromo-2,3-bis((2-ethylhexyl)oxy)-7,8-difluorophenazine(compound 3a)： Compound 2a (3.27g, 6.92 mmol) and NBS(4.93 g, 27.68 mmol) were added to a 250 ml two-necked reaction flask, Then add DMF (30 ml) as a solvent, the mixture was reacted at 85 ℃ for 3 h. The reaction solution was poured into water, and the aqueous phase was extracted with DCM for three times, the crude product was purified by column chromatography using PE/DCM = (3:1, v/v) unfolding agent, with a yield of 70%.

Compound3a： ^{1}H NMR (400 MHz, Chloroform-d) δ 8.06 (t, J = 9.5 Hz, 2H), 4.10 (d, J = 6.2 Hz, 4H), 1.89 (q, J = 6.5 Hz, 2H), 1.70 – 1.63 (m, 2H), 1.30 (d, J = 48.2 Hz, 18H), 1.01 – 0.88 (m, 15H). ^{13}C NMR (101 MHz, Chloroform-d) δ 155.44, 140.84, 139.65, 135.65, 129.25, 115.76, 77.72, 40.30, 29.85, 29.37, 28.80, 23.26, 22.77, 22.36, 13.82, 13.79, 10.82.

Compound3b： ^{1}H NMR (400 MHz, Chloroform-*d*) δ 8.50 (s, 2H), 4.11 (d, *J* = 6.3 Hz, 4H), 1.93 – 1.88 (m, 2H), 1.70 – 1.65 (m, 2H), 1.36 (d, *J* = 7.4 Hz, 12H), 0.98 – 0.90 (m, 11H). ^{13}C NMR (101 MHz, Chloroform-d) δ 155.76, 141.15, 139.96, 135.97, 129.57, 116.07, 78.03, 40.61, 30.16, 29.69, 29.11, 23.58, 23.08, 22.68, 14.13, 14.11, 11.13.

1,4-bis(6-(2-butyloctyl)thieno[3,2-b]thiophen-2-yl)-2,3-bis((2-ethylhexyl)oxy)-7, 8-difluorophenazine(compound 4a)： To a 50 ml two-necked reaction flask was sequentially added compound 3a (193 mg, 306.15 μmol), Pd(PPh3)4 (21.23 mg, 18.37 μmol), then protected by argon, 10 mL of toluene was added as solvent, and using a syringe, tributyl (6-(2-butyloctyl)thieno[3,2-b]thiophen-2-yl) stannane (457.3 mg, 765.37 μmol), followed by stirring the mixture at 110 ℃ for 12 h. When the reaction was complete, the reaction solution was purified by PE over silica gel column to give 298 mg of an orange-yellow oily liquid in a 90% yield.

Compound4a： ^{1}H NMR (400 MHz, Chloroform-*d*) δ 7.97 (s, 2H), 7.93 (d, *J* = 9.3 Hz, 2H), 7.02 (s, 2H), 3.95 (d, *J* = 6.2 Hz, 4H), 2.73 (d, *J* = 7.0 Hz, 4H), 1.95 (s, 2H),

1.72 – 1.66 (m, 2H), 1.31 (d, *J* = 35.5 Hz, 43H), 1.16 (s, 8H), 0.86 (dt, *J* = 22.0, 6.7 Hz, 20H), 0.75 (t, *J* = 7.5 Hz, 6H). ^{13}C NMR (101 MHz, Chloroform-d) δ 154.87, 140.15, 134.39, 134.18, 124.12, 123.94, 122.74, 113.92, 77.86, 40.46, 37.26, 34.96, 33.65, 33.32, 31.90, 30.26, 29.70, 29.67, 29.33, 29.10, 28.85, 26.60, 23.48, 23.05, 22.97, 22.66, 22.65, 14.12, 14.08, 14.05, 10.86.

Compound4b： ^{1}H NMR (400 MHz, Chloroform-*d*) δ 8.38 (s, 2H), 7.97 (s, 2H), 7.03 (s, 2H), 3.96 (d, *J* = 6.2 Hz, 4H), 2.74 (d, *J* = 7.0 Hz, 4H), 1.96 (s, 2H), 1.72 – 1.68 (m, 2H), 1.30 (dd, *J* = 35.6, 10.6 Hz, 60H), 1.17 (s, 12H), 0.86 (dt, *J* = 24.8, 6.7 Hz, 23H), 0.75 (t, *J* = 7.4 Hz, 8H). ^{13}C NMR (101 MHz, Chloroform-d) δ 155.29, 142.74, 140.83, 140.01, 137.99, 134.65, 134.20, 129.73, 124.24, 124.03, 122.83, 77.90, 40.46, 37.27, 34.94, 33.63, 33.30, 31.91, 30.25, 30.12, 29.71, 29.10, 28.86, 26.60, 23.46, 23.07, 22.99, 22.67, 14.17, 14.10, 14.07, 10.87.

5,5'-(2,3-bis((2-ethylhexyl)oxy)-7,8-difluorophenazine-1,4-diyl)bis(3-(2-butyloctyl)thieno[3,2-b]thiophene-2-carbaldehyde)(compound 5a)： Under argon atmosphere, a solution of compound 4a (290 mg, 267.12 μmol), dissolved in 1,2-dichloroethane (8 mL) was added to a 25 mL reaction vial, followed by the addition of the intermediate (0.51 mL of ultra-dry DMF was added to a 10 mL reaction vial under argon atmosphere, $POCl_3$ (0.37 mL) was added dropwise under an ice-water bath, and the intermediates were stirred at room temperature for 1 h. The mixture was reacted at 85 ℃ for 3 h. The reaction solution was quenched with saturated aqueous potassium carbonate, and the aqueous phase was extracted with DCM for three times, Solvent removal by rotary evaporator and purified by column chromatography with the unfolding agent of PE/DCM = (2:1, v/v), to obtain an orange viscous liquid of 260 mg, with a yield of 85%.

Compound5a： ^{1}H NMR (400 MHz, Chloroform-*d*) δ 10.14 (s, 2H), 8.05 (s, 2H), 7.97 – 7.91 (m, 2H), 3.98 (d, *J* = 6.2 Hz, 4H), 3.10 (d, *J* = 7.1 Hz, 4H), 2.04 (s, 2H), 1.69 (t, *J* = 6.3 Hz, 2H), 1.45 – 1.13 (m, 60H), 0.89 – 0.79 (m, 20H), 0.74 (t, *J* = 7.5 Hz, 7H).^{13}C NMR (101 MHz, Chloroform-d) δ 182.74, 155.17, 152.29, 144.69, 143.64, 143.53, 140.87, 139.93, 139.59, 124.35, 124.02, 113.99, 78.37, 40.49, 38.89,

33.77, 33.43, 31.82, 30.23, 29.67, 29.58, 29.33, 29.08, 28.80, 26.61, 23.45, 22.95, 22.59, 14.05, 14.01, 10.82.

Compound5b： ^{1}H NMR (400 MHz, Chloroform-*d*) δ 10.15 (s, 2H), 8.38 (s, 2H), 8.05 (s, 2H), 3.99 (d, *J* = 6.2 Hz, 4H), 3.11 (d, *J* = 7.1 Hz, 4H), 2.04 (s, 2H), 1.72 – 1.68 (m, 2H), 1.25 (s, 100H), 0.92 – 0.78 (m, 38H), 0.75 (t, *J* = 7.4 Hz, 8H).^{13}C NMR (101 MHz, Chloroform-d) δ 182.77, 155.58, 144.73, 143.68, 143.53, 140.73, 140.25, 140.07, 139.95, 135.46, 129.56, 124.40, 124.14, 78.40, 40.48, 38.92, 33.74, 33.40, 31.91, 31.82, 30.22, 30.02, 29.68, 29.58, 29.34, 29.08, 28.80, 26.59, 23.43, 22.96, 22.67, 22.60, 14.08, 14.05, 14.03, 10.82.

2,2'-((2Z,2'Z)-(((2,3-bis((2-ethylhexyl)oxy)-7,8-difluorophenazine-1,4-diyl)bis(3-(2-butyloctyl)thieno[3,2-b]thiophene-5,2-diyl))bis(methaneylylidene))bis(5,6-difluoro-3-oxo-2,3-dihydro-1H-indene-2,1-diylidene))dimalononitrile(FQ-4F)： Under argon atmosphere, compound 5a (126 mg, 110.36 μmol) and 2-(5,6-difluoro-3-oxo-2,3-dihydro-1H-inden-1-ylidene)malononitrile (116.14 mg, 441.45 μmol), added chloroform/pyridine = (50:1, v/v) mixed solution (5 mL : 0.1 mL), the mixture was reacted at 65 ℃ for 5 h, and then settled in methanol, filtration, the filter cake continued to be precipitated twice with a mixture of EA/MeOH = (7:1, v/v) solution, and finally the EA was recrystallized to obtain 90 mg, with a yield of 50%. The same method was used to obtain FQ-FCl and FQ-4Cl, with yield of 65% and 62%, respectively.

FQ-4F: ^{1}H NMR (400 MHz, Chloroform-*d*) δ 9.13 (s, 2H), 8.52 (dd, *J* = 10.0, 6.4 Hz, 2H), 8.28 (s, 2H), 7.97 (t, *J* = 9.1 Hz, 2H), 7.69 (t, *J* = 7.4 Hz, 2H), 4.07 (d, *J* = 5.9 Hz, 4H), 3.17 (d, *J* = 7.2 Hz, 4H), 2.06 (s, 2H), 1.79 (s, 2H), 1.50 – 1.17 (m, 53H), 0.83 (dt, *J* = 23.7, 7.7 Hz, 26H). ^{13}C NMR (101 MHz, Chloroform-d) δ 185.70, 159.25, 155.55, 153.14, 153.00, 152.22, 150.33, 144.68, 144.67, 139.14, 138.86, 136.37, 135.85, 124.53, 123.94, 121.01, 114.89, 114.70, 114.40, 112.67, 112.49, 76.98, 69.30, 40.53, 39.73, 35.00, 33.56, 33.28, 31.83, 30.28, 29.59, 29.10, 28.94, 26.69, 23.54, 23.01, 22.94, 22.60, 14.05, 14.02, 10.86.

FQ-FCl: ^{1}H NMR (400 MHz, Chloroform-*d*) δ 9.12 (s, 2H), 8.69 (s, 2H), 8.34 (s, 2H), 7.98 – 7.92 (m, 4H), 4.10 (d, *J* = 5.8 Hz, 4H), 3.17 (d, *J* = 7.1 Hz, 4H), 2.05 (s,

2H), 1.82 (s, 2H), 1.22 (s, 62H), 0.82 (s, 28H). ^{13}C NMR (101 MHz, Chloroform-d) δ 159.04, 155.67, 152.53, 150.72, 145.02, 144.89, 139.46, 138.42, 136.85, 136.20, 136.09, 126.70, 125.09, 124.60, 123.90, 120.92, 114.98, 114.39, 76.97, 40.56, 39.79, 35.03, 33.58, 33.29, 31.83, 30.30, 29.59, 29.10, 28.95, 26.71, 23.57, 23.02, 22.94, 22.60, 14.05, 14.02, 10.88.

FQ-4Cl: ^{1}H NMR (400 MHz, Chloroform-*d*) δ 9.09 (s, 2H), 8.66 (s, 2H), 8.37 (s, 4H), 7.93 (s, 2H), 4.13 (d, *J* = 5.8 Hz, 4H), 3.16 (d, *J* = 7.0 Hz, 4H), 2.03 (s, 2H), 1.85 (s, 2H), 1.51 – 1.15 (m, 65H), 0.91 – 0.76 (m, 29H). ^{13}C NMR (101 MHz, Chloroform-d) δ 185.70, 158.91, 156.11, 152.53, 150.69, 145.01, 144.91, 139.54, 139.46, 139.42, 139.22, 138.34, 136.72, 136.26, 136.14, 136.04, 129.20, 126.60, 125.03, 124.67, 123.95, 120.87, 114.97, 114.37, 76.98, 69.11, 40.57, 39.81, 35.01, 33.55, 33.24, 31.80, 30.30, 29.68, 29.57, 29.10, 28.92, 26.67, 23.58, 23.03, 22.92, 22.60, 14.05, 10.89.

2.4 Synthetic details of seven materials out of ten

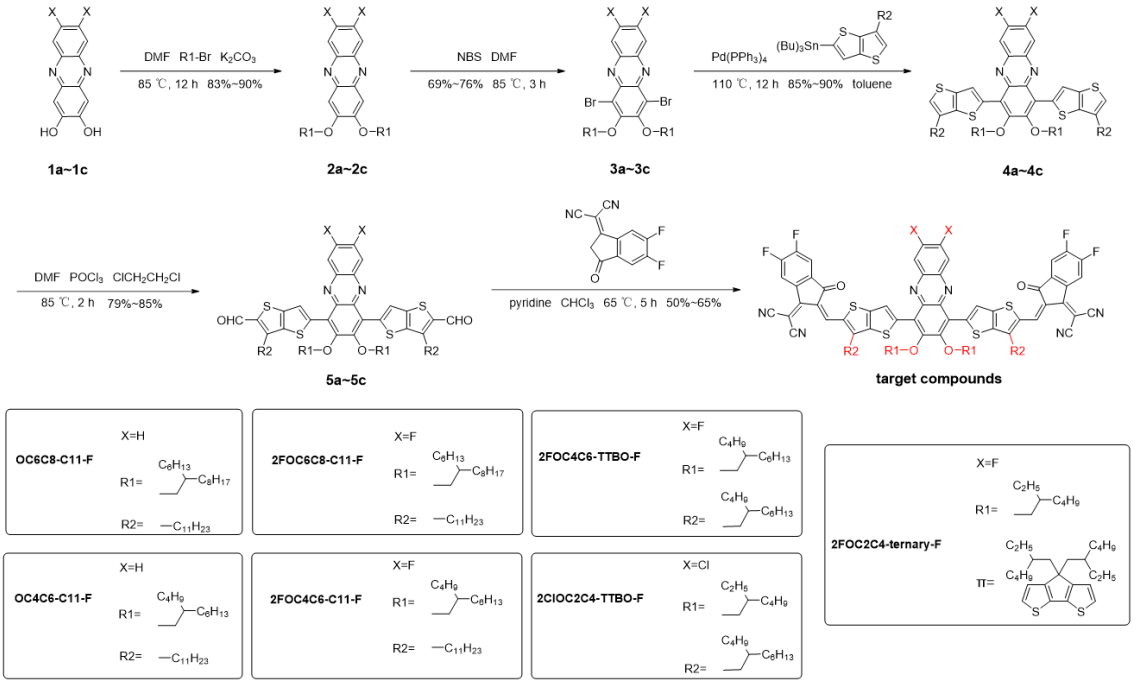

Scheme S2. Synthetic routes of seven materials out of ten.

3. Supporting Figures

3.1 Film absorption of seven molecules.

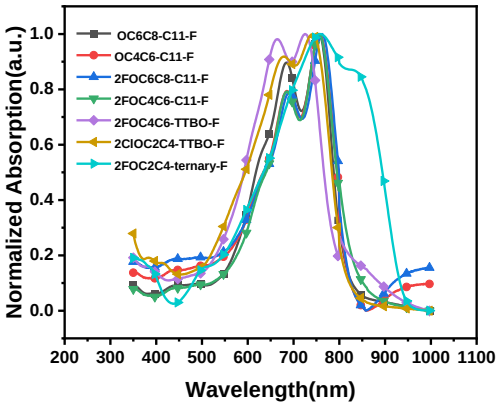

Fig. S2 Thin films absorption spectra of seven NFRAs.

3.2 Photovoltaic properties of seven molecules.

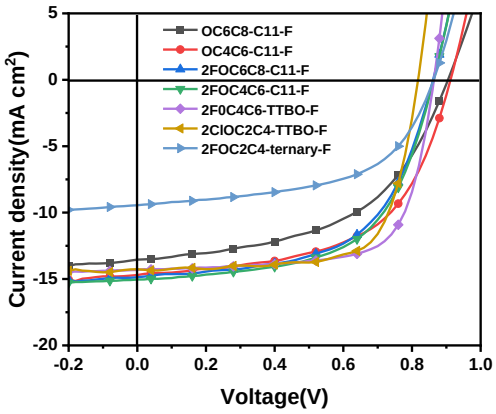

Fig. S3 *J*–*V* curves of OSCs based on PM6:seven NFRAs, respectively.

3.3 Fluorescence spectrum of FQ-4F, FQ-FCl and FQ-4Cl.

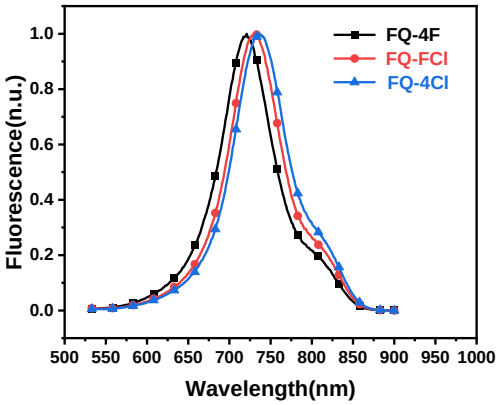

Fig. S4 Fluorescence spectra in $CHCl_3$ solutions (1×10^{-5} M) .

3.4 Cyclic voltammograms of FQ-4F, FQ-FCl and FQ-4Cl.

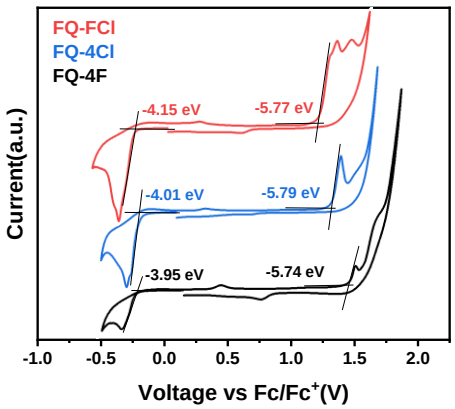

Fig. S5 Cyclic voltammograms of FQ-4F, FQ-FCl and FQ-4Cl.

3.5 TGA curves of FQ-4F, FQ-FCl and FQ-4Cl.

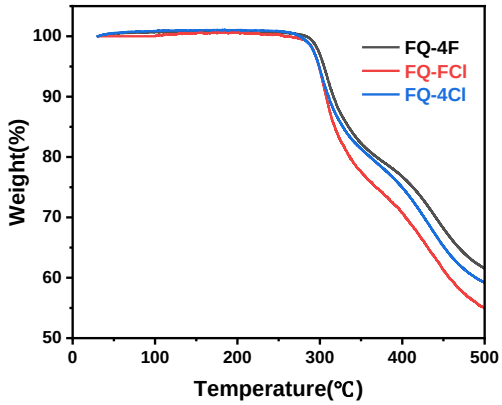

Fig. S6 TGA curves of FQ-4F, FQ-FCl and FQ-4Cl.

3.6 DFT calculations of FQ-4F, FQ-FCl and FQ-4Cl.

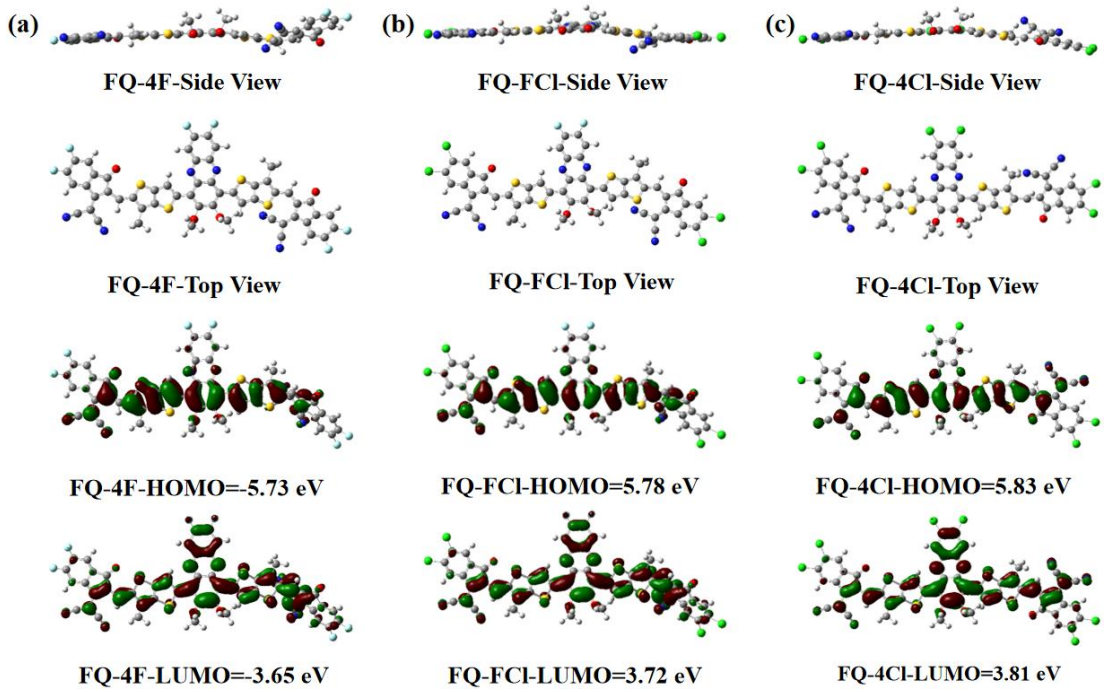

Fig. S7 Side views, top views and frontier molecular orbitals of (a) FQ-4F, (b) FQ-FCl and (c) FQ-4Cl by DFT calculations.

3.7 Photostability of FQ-4F, FQ-FCl and FQ-4Cl processed OSCs.

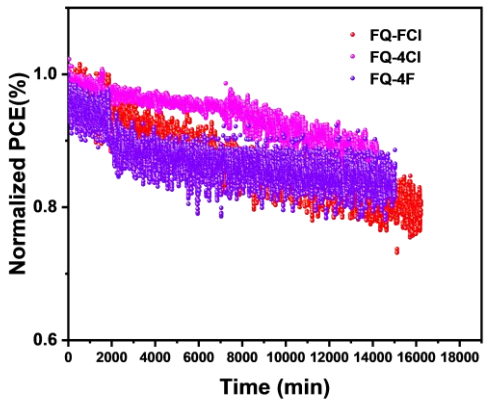

Fig. S8 Photostability of FQ-4F, FQ-FCl and FQ-4Cl processed OSCs.

4. Supporting Tables

4.1 The optical and photovoltaic properties of seven NFREAs

Table S1. Optical properties of seven NFREAs.

Acceptors	λ_{max}^{film} (nm)	λ_{edge} (nm)	E_g^{opt} (eV)	LUMO (eV)	HOMO (eV)
OC6C8-C11-F	755	815	1.52	-3.88	-5.71
OC4C6-C11-F	756	844	1.45	-3.87	-5.59
2FOC6C8-C11-F	762	831	1.49	-3.88	-5.51
2FOC4C6-C11-F	756	842	1.47	-3.75	-5.57
2FOC4C6-TTBO-F	725	810	1.53	-3.86	-5.61
2ClOC2C4-TTBO-F	741	814	1.52	-3.99	-5.76
2FOC2C4-ternary-F	835	961	1.29	-3.89	-5.34

Table S2. Photovoltaic performance of OSCs based on PM6:seven NFREAs, respectively measured under the illumination of AM 1.5 G at 100 mW cm^{-2}.

Devices based on PM6	V_{OC}(V)	J_{SC}(mA cm^{-2})	FF(%)	PCE(%)
OC6C8-C11-F	0.90	13.54	51.87	6.37
OC4C6-C11-F	0.91	14.69	57.00	7.66
2FOC6C8-C11-F	0.86	15.26	58.44	7.72
2FOC4C6-C11-F	0.86	15.04	59.08	7.67
2FOC4C6-TTBO-F	0.86	14.32	70.83	8.77
2ClOC2C4-TTBO-F	0.82	14.26	71.55	8.35
2FOC2C4-ternary-F	0.86	9.44	55.80	4.55

4.2 Optimization of device conditions based on PM6:FQ-4F

Table S3. Photovoltaic properties of the OSCs based on PM6:FQ-4F (D:A=1:1.2) with different concentration.

C(mg/mL)	V_{OC}(V)	J_{SC}(mA cm^{-2})	FF(%)	PCE[a](%)
14.3	0.84	14.26	72.35	8.72
15.4	0.84	13.97	72.12	8.44
16.5	0.82	14.35	69.57	8.17

[a] Under the illumination of AM 1.5G, 100 mW cm^{-2}.

Table S4. Photovoltaic properties of the OSCs based on PM6:FQ-4F (D:A=1:1.2, C=14.3 mg/mL) with different Rotating speed.

Rotating speed	V_{OC}(V)	J_{SC}(mA cm^{-2})	FF(%)	PCE[a](%)
2000r	0.85	13.73	73.13	8.46
2500r	0.84	14.78	72.15	8.93
3000r	0.85	14.49	73.86	9.02

[a] Under the illumination of AM 1.5G, 100 mW cm^{-2}.

Table S5. Photovoltaic properties of the OSCs based on PM6:FQ-4F (D:A=1:1.2, C=14.3 mg/mL, 3000 rpm) with different annealing temperature.

Annealing temperature	V_{OC}(V)	J_{SC}(mA cm^{-2})	FF(%)	PCE[a](%)
90 ℃	0.85	14.87	73.88	9.25
100 ℃	0.85	14.49	73.86	9.02
110 ℃	0.85	14.04	72.11	8.57

[a] Under the illumination of AM 1.5G, 100 mW cm^{-2}.

Table S6. Photovoltaic properties of the OSCs based on PM6:FQ-4F (D:A=1:1.2, C=14.3 mg/mL, 3000 rpm, 90 ℃) with different CN ratio.

Additives	V_{OC}(V)	J_{SC}(mA cm^{-2})	FF(%)	PCE[a](%)
0.25%	0.85	13.74	69.04	8.07
0.5%	0.85	14.68	74.44	9.33
0.75%	0.84	12.14	66.20	6.74

[a] Under the illumination of AM 1.5G, 100 mW cm^{-2}.

4.3 Optimization of device conditions based on PM6:FQ-FCl

Table S7. Photovoltaic properties of the OSCs based on PM6:FQ-FCl (D:A=1:1.2) with different concentration.

C(mg/mL)	V_{OC}(V)	J_{SC}(mA cm^{-2})	FF(%)	PCE[a](%)
14.3	0.82	15.12	70.47	8.72
15.4	0.82	14.34	72.45	8.55
16.5	0.82	14.18	71.93	8.39

[a] Under the illumination of AM 1.5G, 100 mW cm^{-2}.

Table S8. Photovoltaic properties of the OSCs based on PM6:FQ-FCl (D:A=1:1.2, C=14.3 mg/mL) with different Rotating speed.

Rotating speed	V_{OC}(V)	J_{SC}(mA cm^{-2})	FF(%)	PCE[a](%)
2000r	0.81	14.27	73.75	8.64
2500r	0.81	15.69	73.73	9.50
3000r	0.82	15.00	74.95	9.29

[a] Under the illumination of AM 1.5G, 100 mW cm^{-2}.

Table S9. Photovoltaic properties of the OSCs based on PM6:FQ-FCl (D:A=1:1.2, C=14.3 mg/mL, 2500 rpm) with different annealing temperature.

Annealing temperature	V_{OC}(V)	J_{SC}(mA cm^{-2})	FF(%)	PCE[a](%)
90 ℃	0.82	14.80	72.33	8.88
100 ℃	0.82	15.58	73.05	9.43
110 ℃	0.82	14.94	73.09	9.02

[a] Under the illumination of AM 1.5G, 100 mW cm^{-2}.

Table S10. Photovoltaic properties of the OSCs based on PM6:FQ-FCl (D:A=1:1.2, C=14.3 mg/mL, 3000 rpm, 100 ℃) with different CN ratio.

Additives	V_{OC}(V)	J_{SC}(mA cm^{-2})	FF(%)	PCE[a](%)
0.25%	0.83	12.93	63.85	6.86
0.5%	0.82	14.53	69.61	8.23
0.75%	0.82	13.32	72.13	7.87

[a] Under the illumination of AM 1.5G, 100 mW cm^{-2}.

4.4 Optimization of device conditions based on PM6:FQ-4Cl

Table S11. Photovoltaic properties of the OSCs based on PM6:FQ-4Cl (D:A=1:1.2) with different concentration.

C(mg/mL)	V_{OC}(V)	J_{SC}(mA cm^{-2})	FF(%)	PCE[a](%)
14.3	0.81	16.24	73.30	9.65
15.4	0.81	16.22	74.55	9.80
16.5	0.80	15.51	70.76	8.87

[a] Under the illumination of AM 1.5G, 100 mW cm^{-2}.

Table S12. Photovoltaic properties of the OSCs based on PM6:FQ-4Cl (D:A=1:1.2, C=15.4 mg/mL) with different Rotating speed.

Rotating speed	V_{OC}(V)	J_{SC}(mA cm^{-2})	FF(%)	PCE[a](%)
2000r	0.80	14.53	68.18	7.90
2500r	0.81	15.30	70.57	8.72
3000r	0.81	15.53	73.28	9.22

[a] Under the illumination of AM 1.5G, 100 mW cm^{-2}.

Table S13. Photovoltaic properties of the OSCs based on PM6:FQ-4Cl (D:A=1:1.2, C=14.3 mg/mL, 3000 rpm) with different annealing temperature.

Annealing temperature	V_{OC}(V)	J_{SC}(mA cm^{-2})	FF(%)	PCE[a](%)
90 ℃	0.82	14.85	72.18	8.74
100 ℃	0.81	15.53	73.28	9.22
110 ℃	0.81	14.50	72.98	8.56

[a] Under the illumination of AM 1.5G, 100 mW cm^{-2}.

Table S14. Photovoltaic properties of the OSCs based on PM6:FQ-4Cl (D:A=1:1.2, C=14.3 mg/mL, 3000 rpm, 100 ℃) with different CN ratio.

Additives	V_{OC}(V)	J_{SC}(mA cm^{-2})	FF(%)	PCE[a](%)
0.25%	0.82	14.08	69.09	7.98
0.5%	0.81	16.87	74.43	10.11
0.75%	0.80	16.35	73.28	9.68

[a] Under the illumination of AM 1.5G, 100 mW cm^{-2}.

5. ^{1}H NMR and ^{13}C NMR spectra

5.1 ^{1}H NMR and ^{13}C NMR spectra of the intermediates and target molecules of FQ-4F, FQ-FCl, and FQ-4Cl

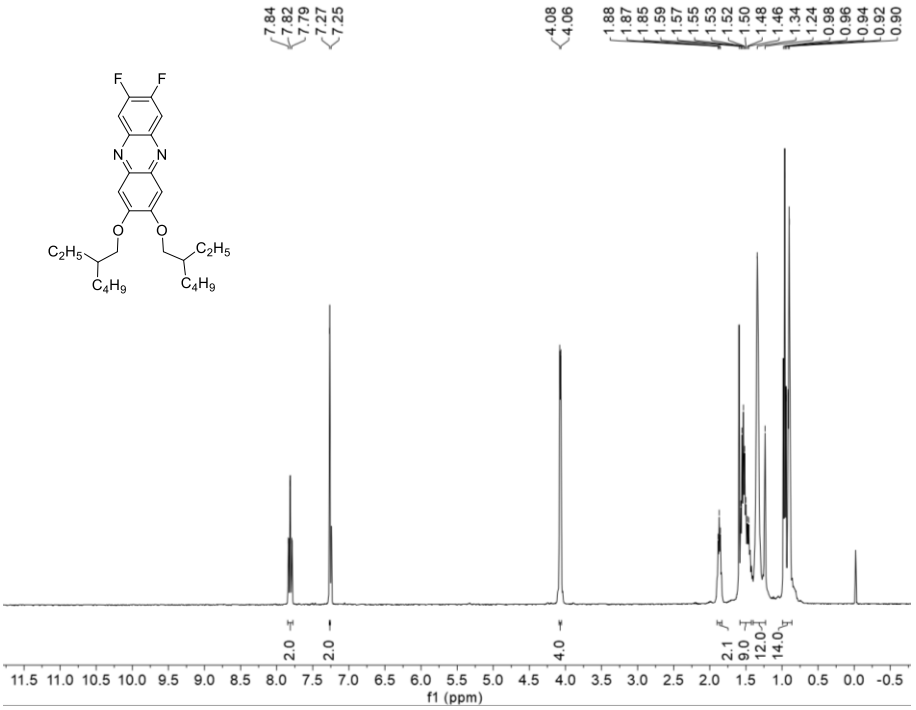

Fig. S9 ^{1}H NMR spectrum of compound 2a in $CDCl_3$.

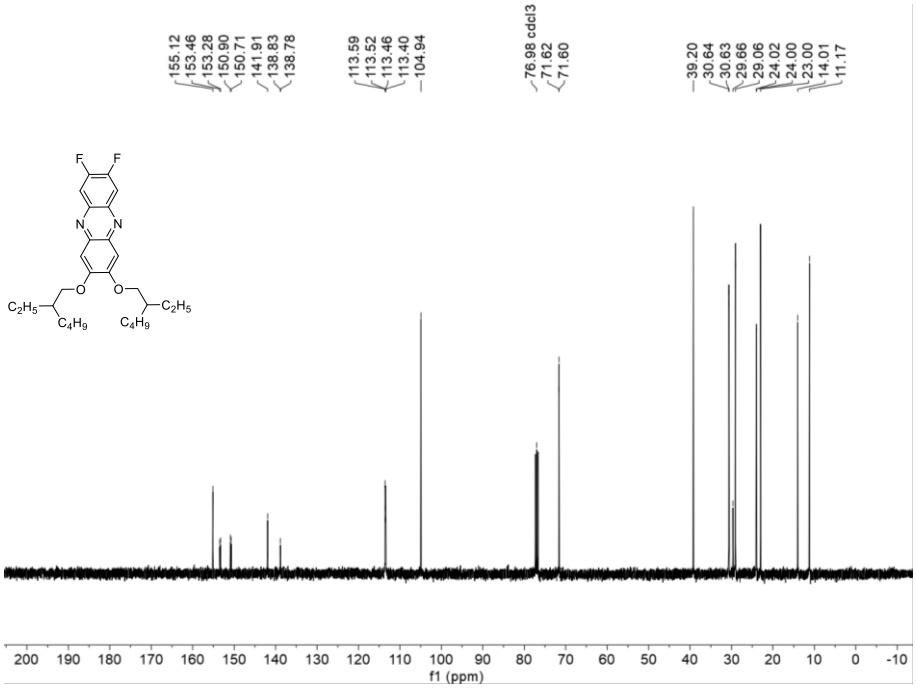

Fig. S10 ^{13}C NMR spectrum of compound 2a in $CDCl_3$.

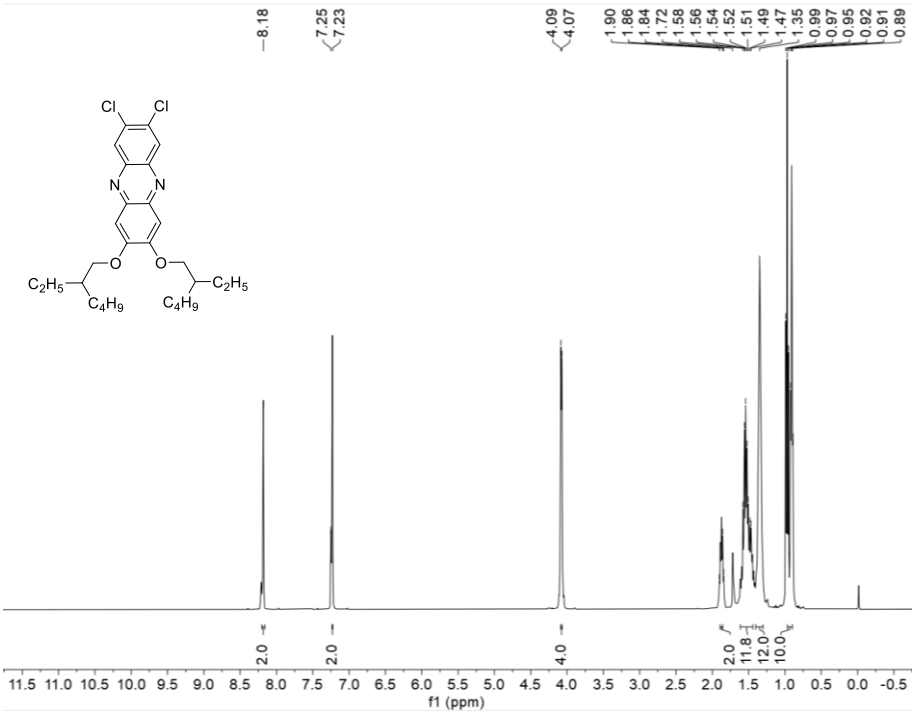

Fig. S11 ^{1}H NMR spectrum of compound 2b in $CDCl_3$.

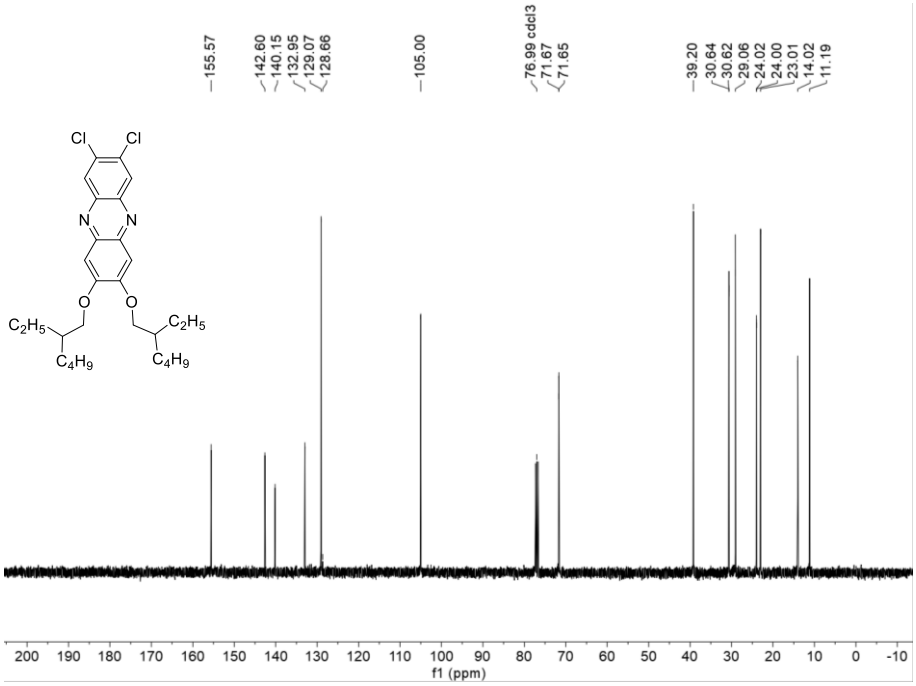

Fig. S12 ^{13}C NMR spectrum of compound 2b in $CDCl_3$.

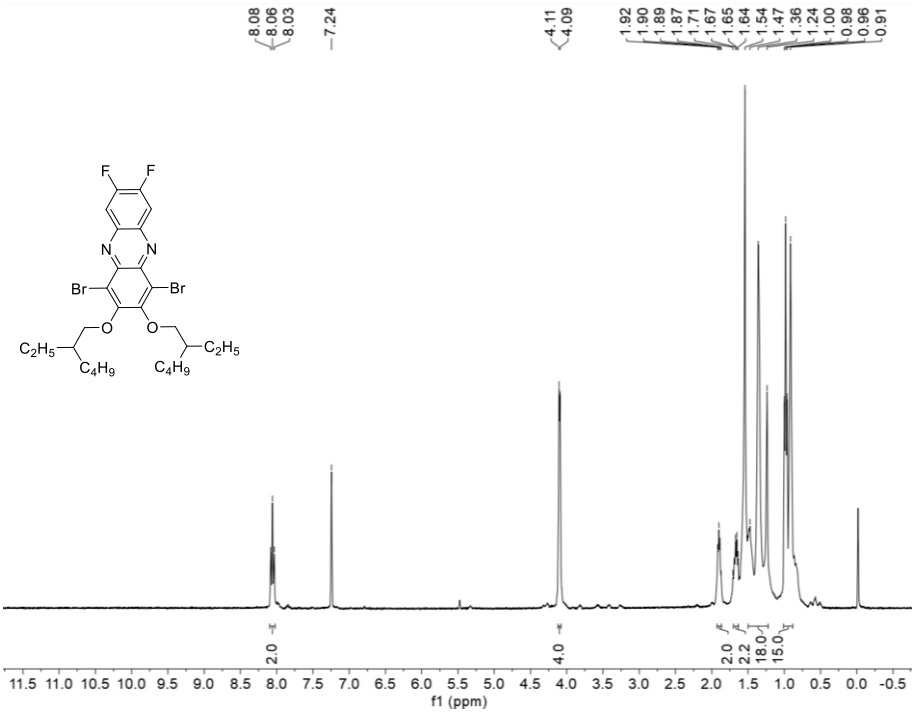

Fig. S13 ^{1}H NMR spectrum of compound 3a in $CDCl_3$.

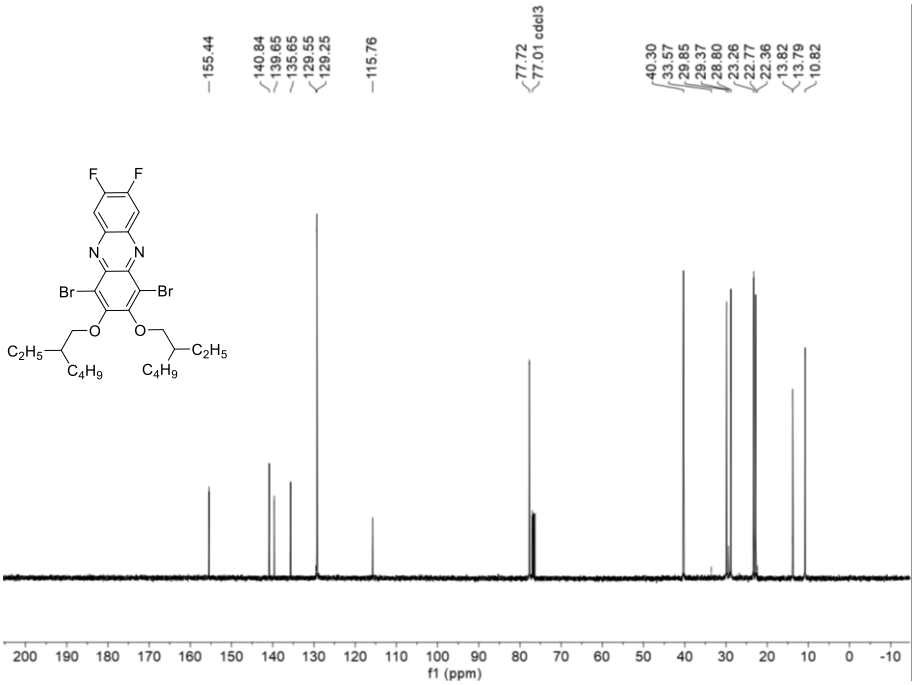

Fig. S14 ^{13}C NMR spectrum of compound 3a in $CDCl_3$.

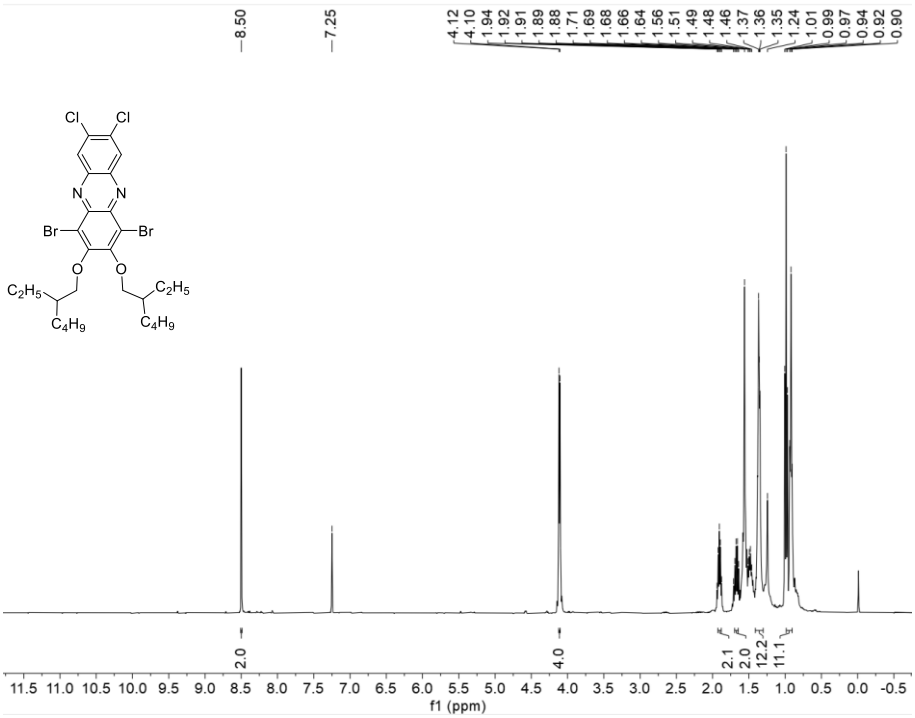

Fig. S15 ^{1}H NMR spectrum of compound 3b in $CDCl_3$.

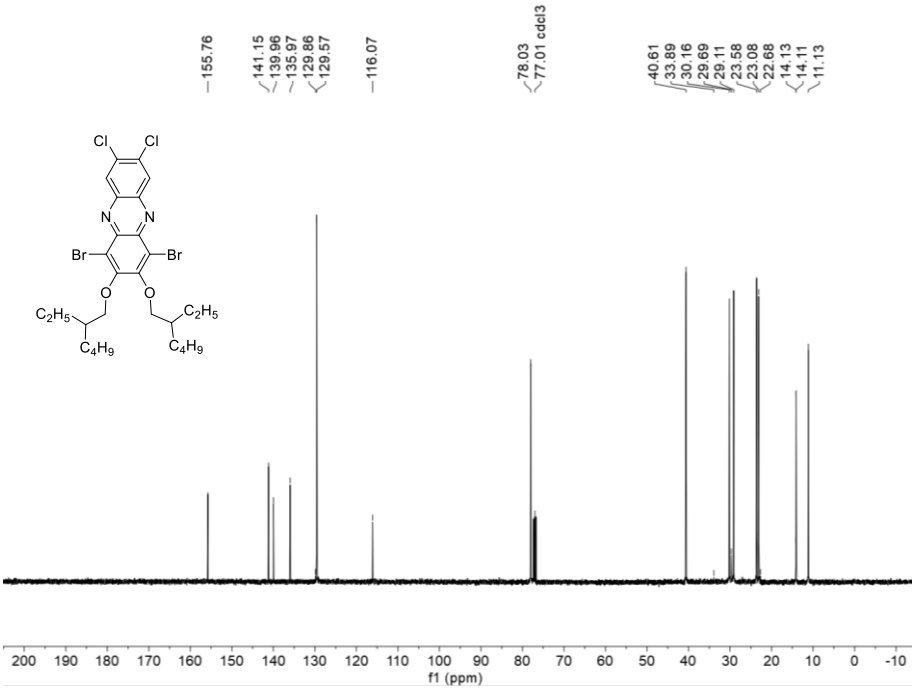

Fig. S16 ^{13}C NMR spectrum of compound 3b in $CDCl_3$.

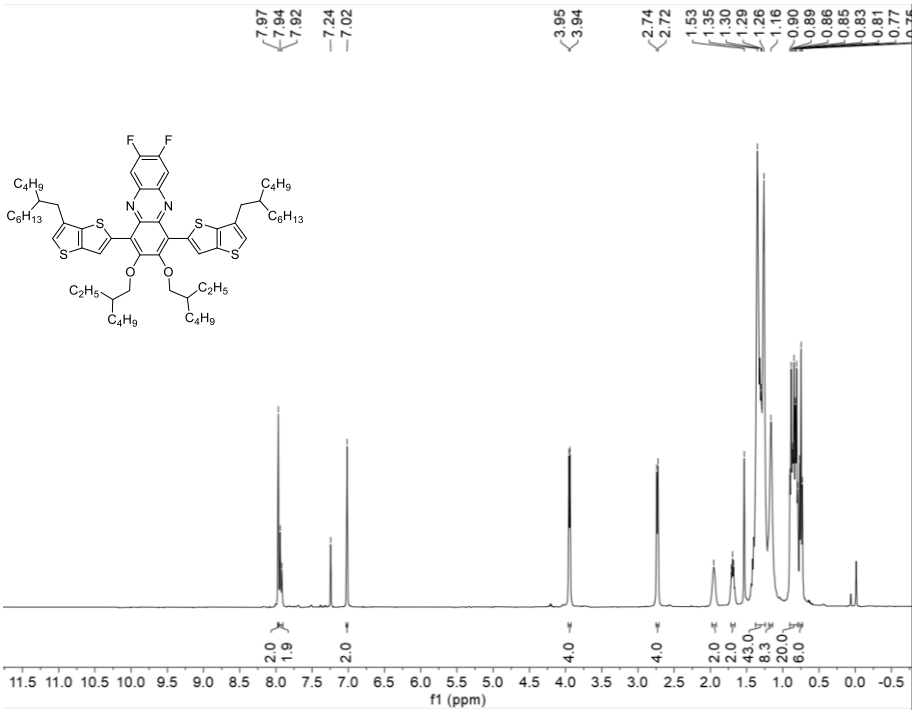

Fig. S17 ^{1}H NMR spectrum of compound 4a in $CDCl_3$.

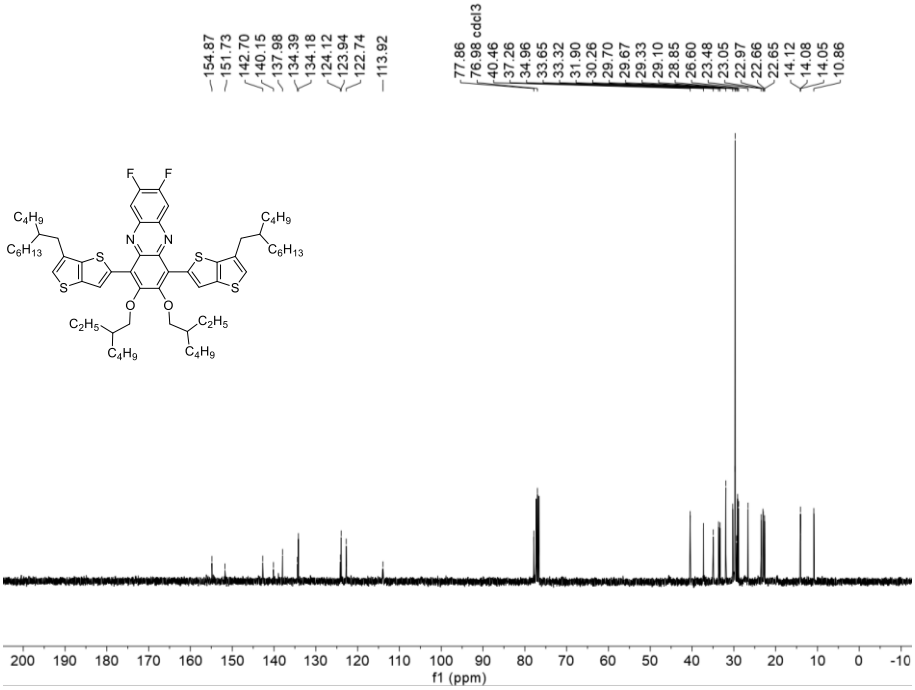

Fig. S18 ^{13}C NMR spectrum of compound 4a in $CDCl_3$.

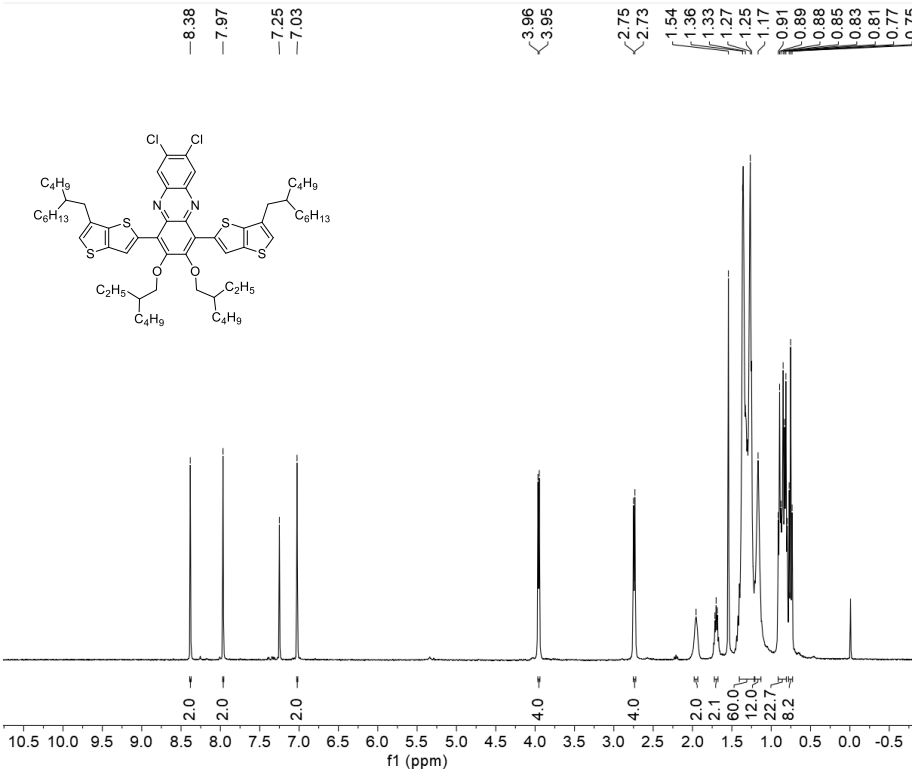

Fig. S19 ^{1}H NMR spectrum of compound 4b in $CDCl_3$.

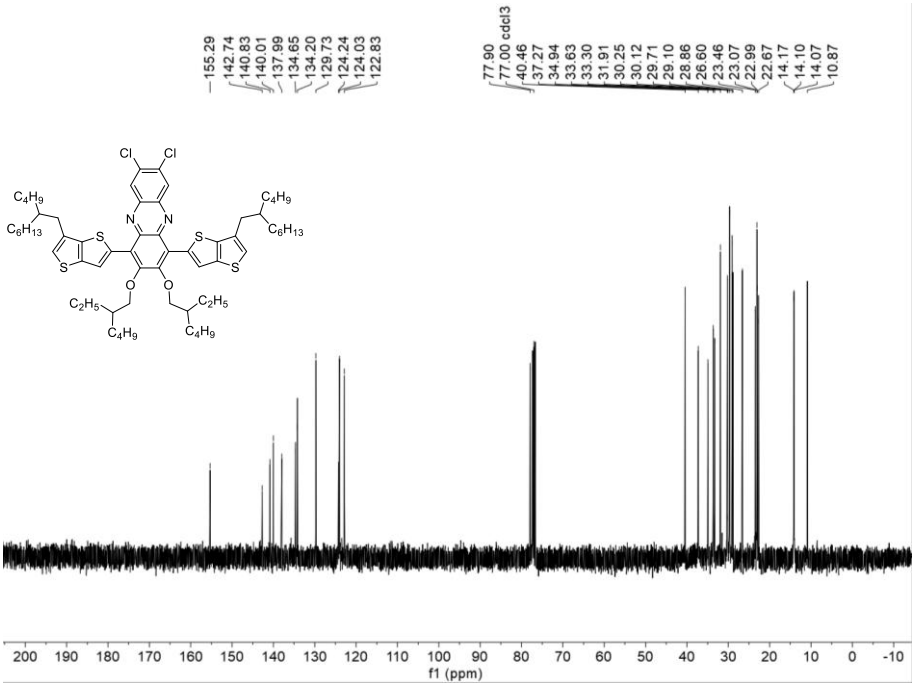

Fig. S20 ^{13}C NMR spectrum of compound 4b in $CDCl_3$.

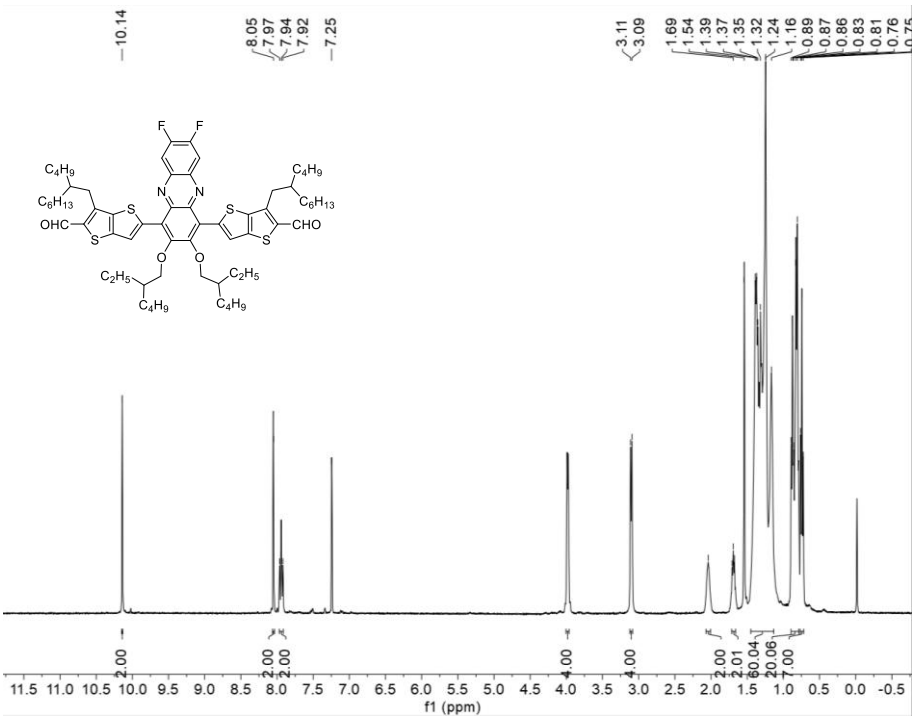

Fig. S21 ^{1}H NMR spectrum of compound 5a in $CDCl_3$.

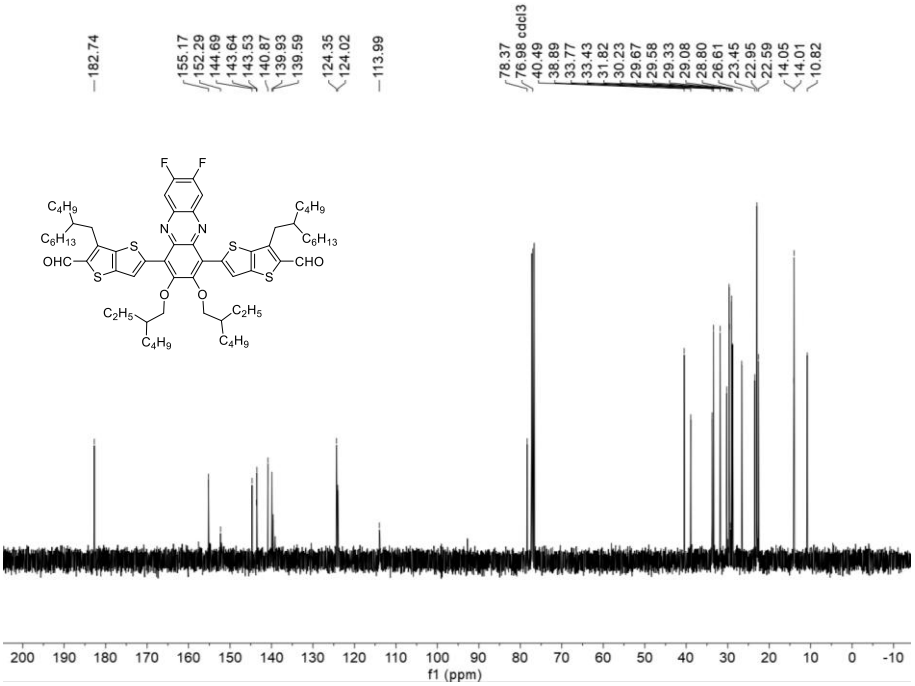

Fig. S22 ^{13}C NMR spectrum of compound 5a in $CDCl_3$.

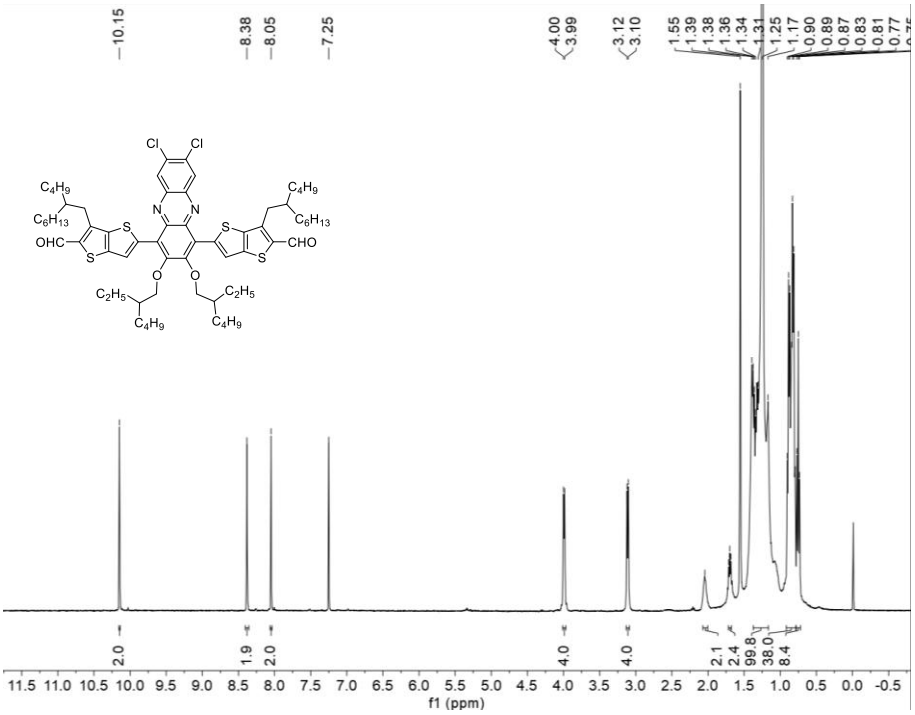

Fig. S23 ^{1}H NMR spectrum of compound 5b in $CDCl_3$.

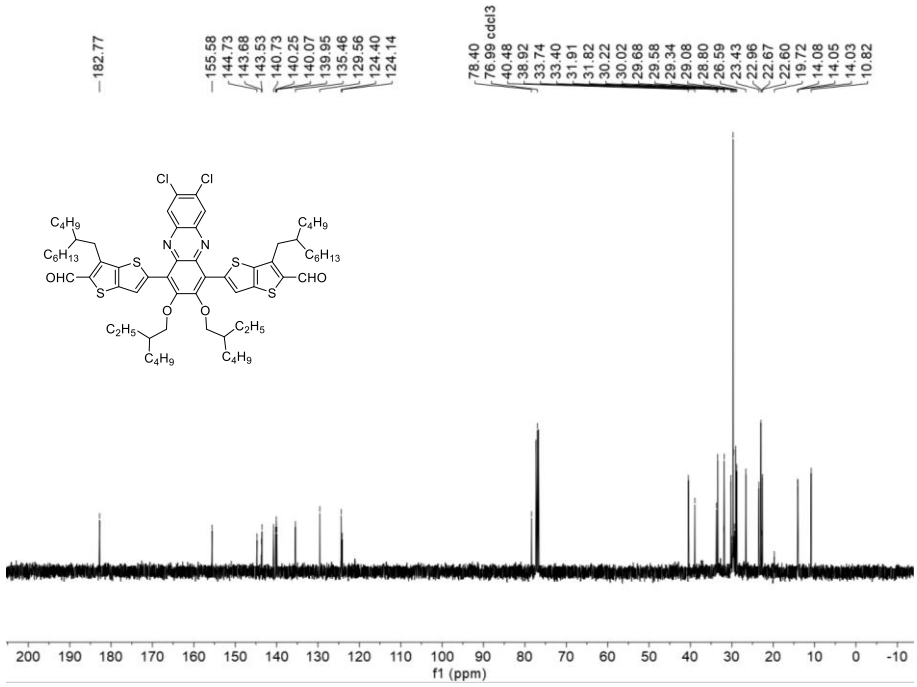

Fig. S24 ^{13}C NMR spectrum of compound 5b in $CDCl_3$.

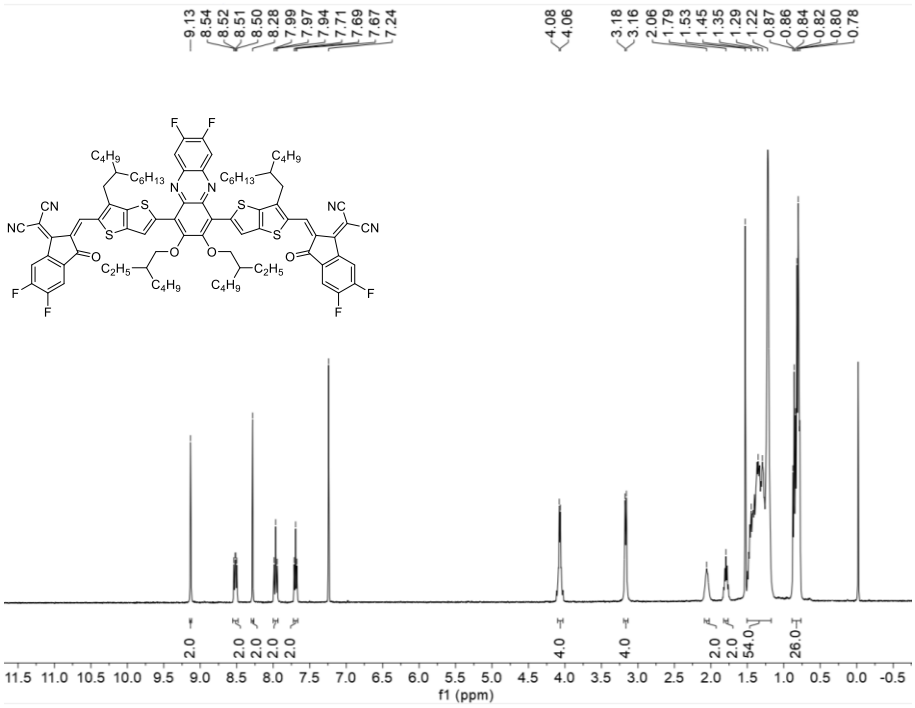

Fig. S25 ^{1}H NMR spectrum of FQ-4F in $CDCl_3$.

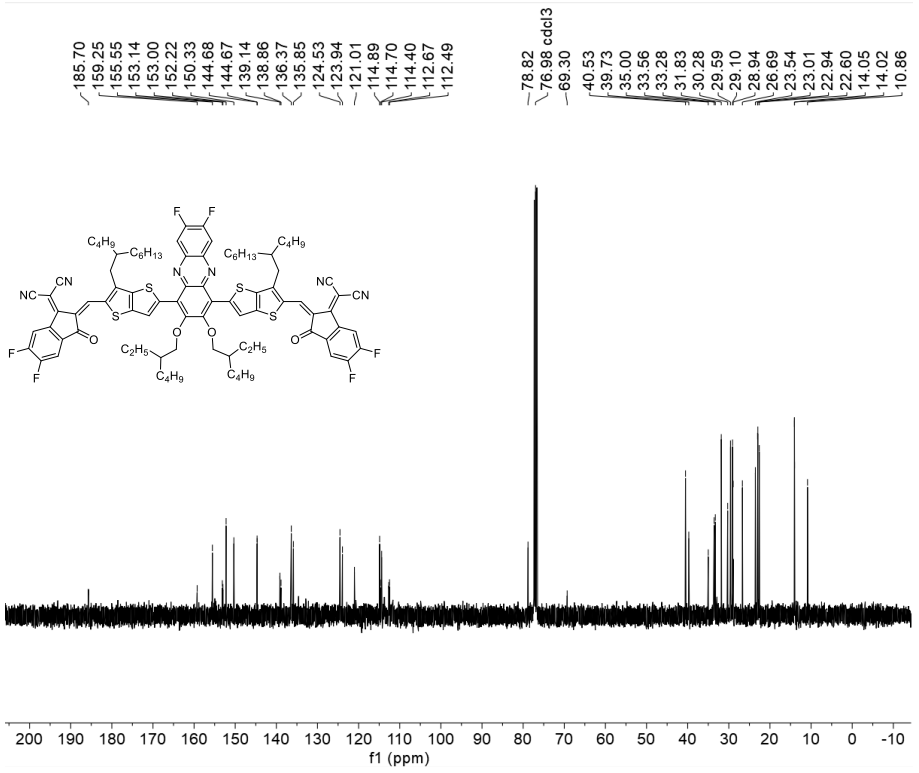

Fig. S26 ^{13}C NMR spectrum of FQ-4F in $CDCl_3$.

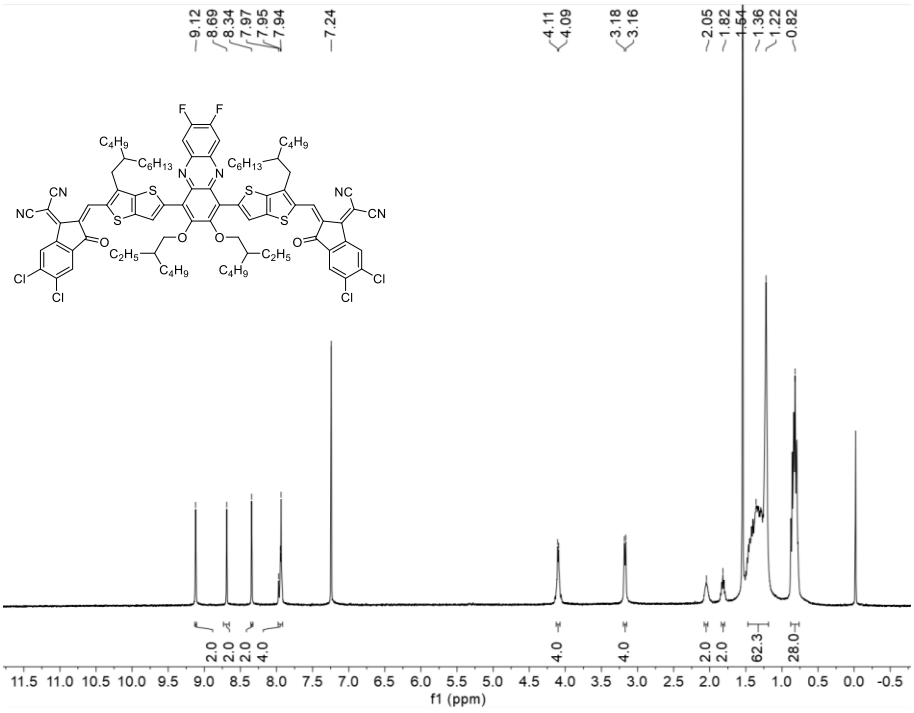

Fig. S27 ^{1}H NMR spectrum of FQ-FCl in $CDCl_3$.

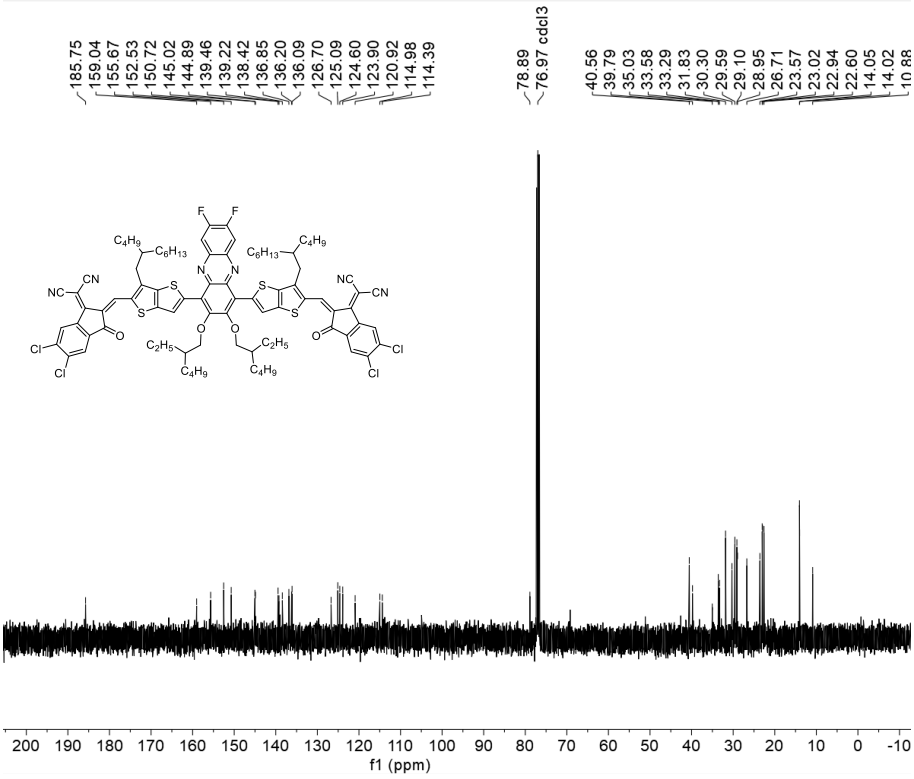

Fig. S28 ^{13}C NMR spectrum of FQ-FCl in $CDCl_3$.

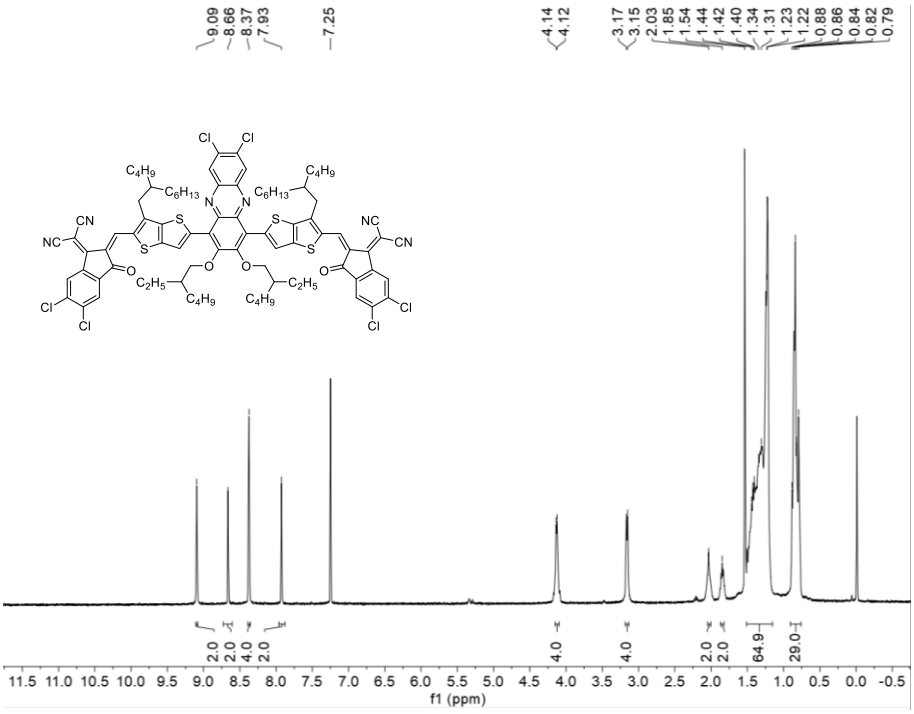

Fig. S29 ^{1}H NMR spectrum of FQ-4Cl in $CDCl_3$.

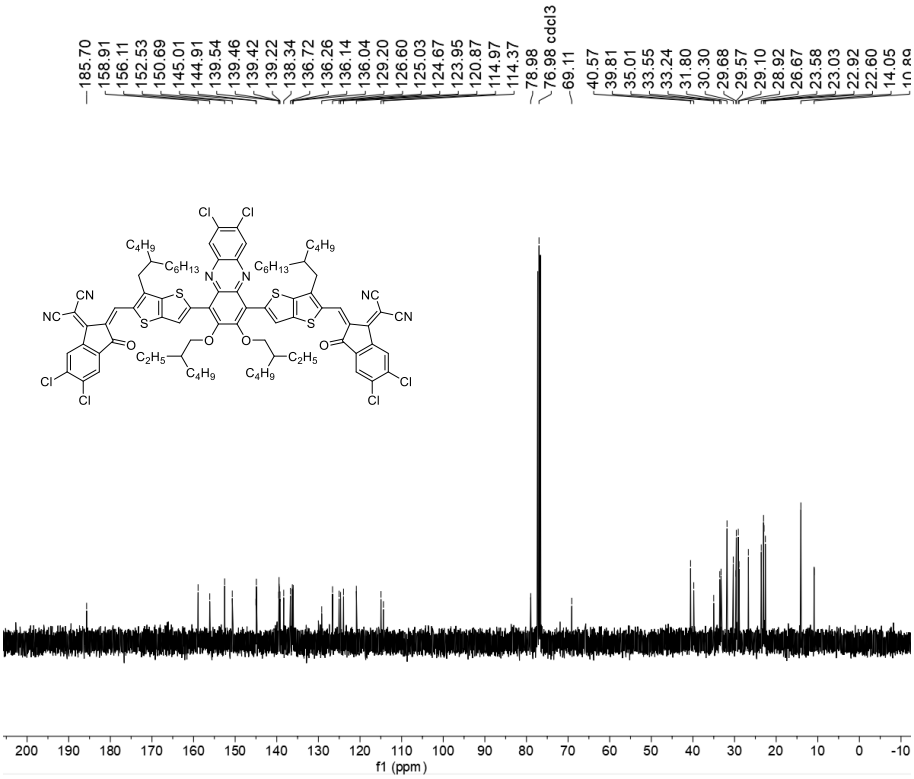

Fig. S30 ^{13}C NMR spectrum of FQ-4Cl in $CDCl_3$.

5.2 ^{1}H NMR spectra of the seven molecules out of ten

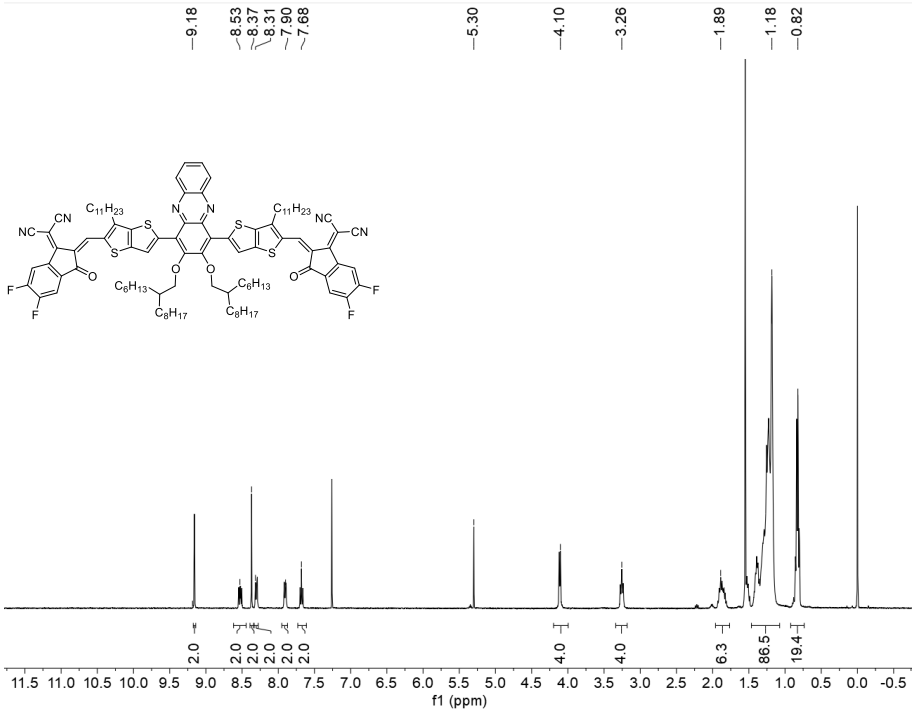

Fig. S31 ^{1}H NMR spectrum of OC6C8-C11-F in $CDCl_3$.

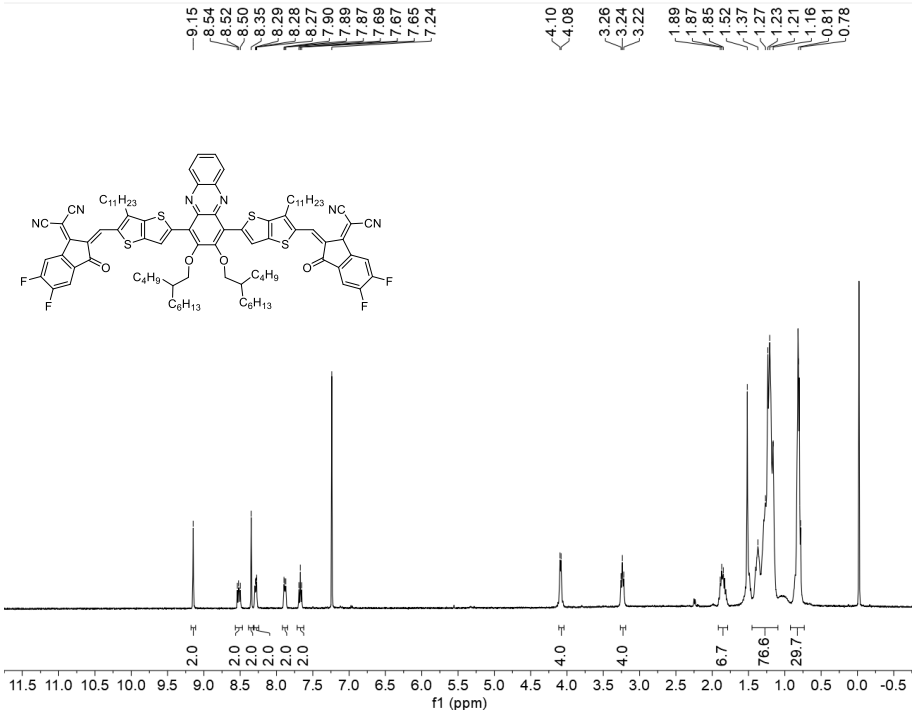

Fig. S32 ^{1}H NMR spectrum of OC4C6-C11-F in $CDCl_3$.

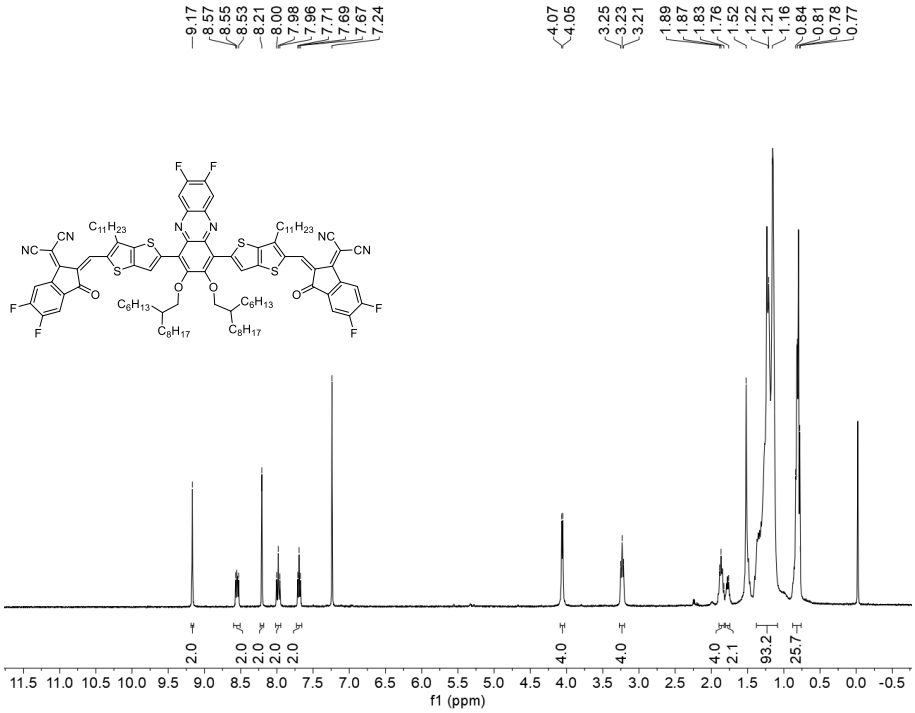

Fig. S33 ^{1}H NMR spectrum of 2FOC6C8-C11-F in $CDCl_3$.

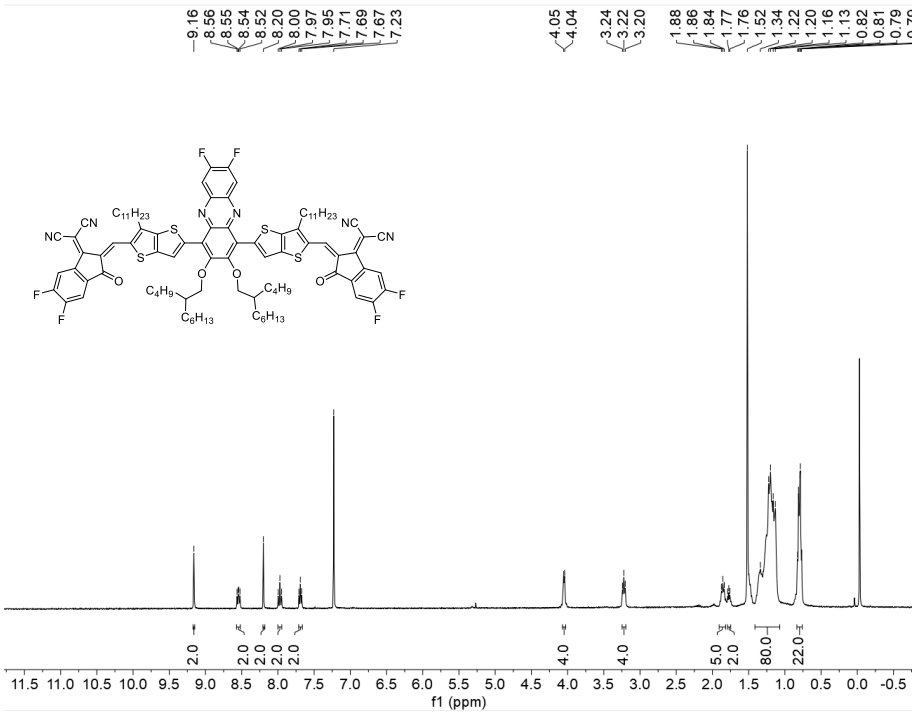

Fig. S34 ^{1}H NMR spectrum of 2FOC4C6-C11-F in $CDCl_3$.

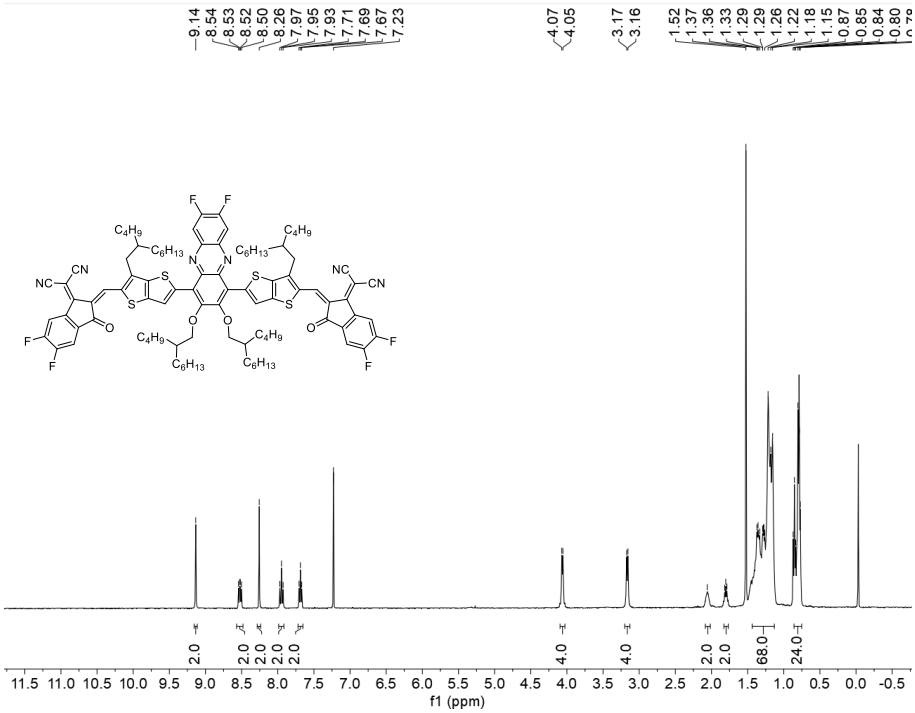

Fig. S35 ^{1}H NMR spectrum of 2FOC4C6-TTBO-F in $CDCl_3$.

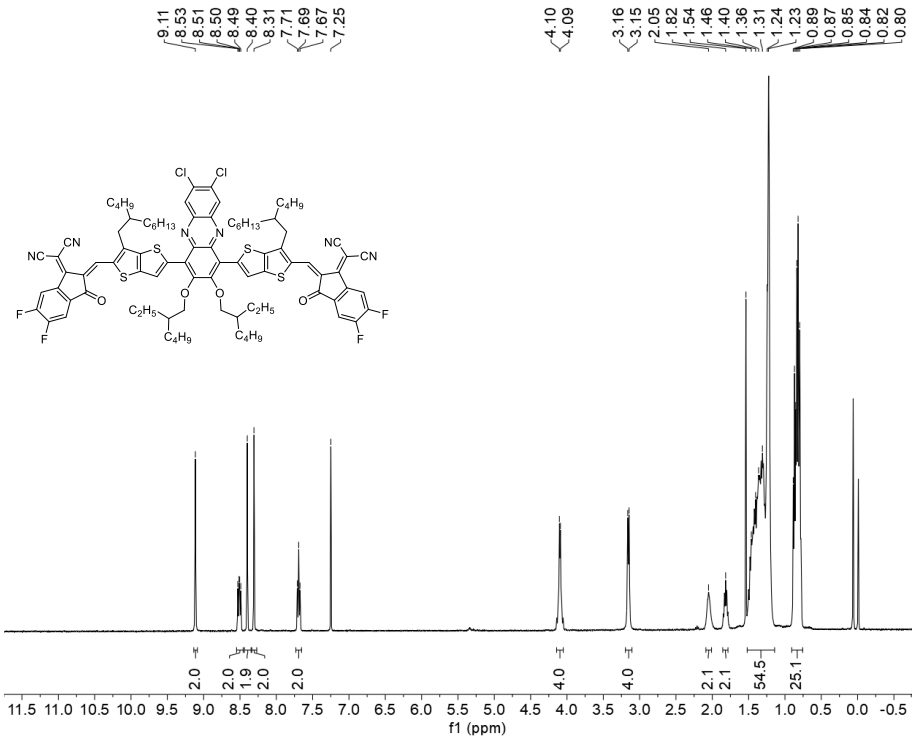

Fig. S36 ^{1}H NMR spectrum of 2ClOC2C4-TTBO-F in $CDCl_3$.

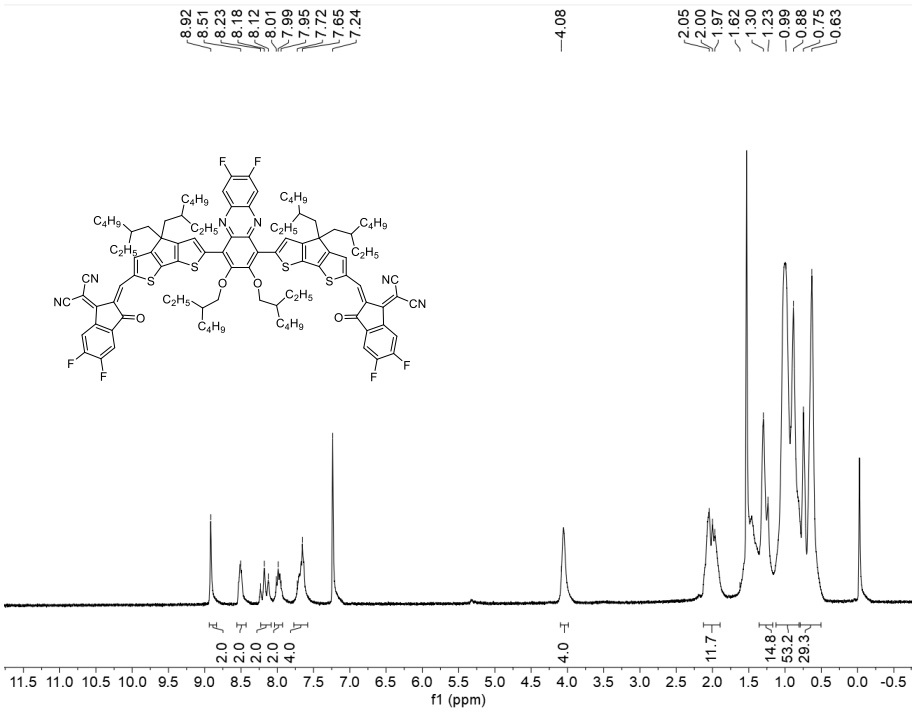

Fig. S37 ^{1}H NMR spectrum of 2FOC2C4-ternary-F in $CDCl_3$.

6. References

1. Z. Yao, X. Liao, K. Gao, F. Lin, X. Xu, X. Shi, L. Zuo, F. Liu, Y. Chen and A. K. Y. Jen, *J. Am. Chem. Soc.*, 2018, **140**, 2054-2057.
2. V. D. Mihailetchi, H. X. Xie, B. de Boer, L. J. A. Koster and P. W. M. Blom, *Adv. Funct. Mater.*, 2006, **16**, 699-708.
3. Z. Zhang, Y. Li, G. Cai, Y. Zhang, X. Lu and Y. Lin, *J. Am. Chem. Soc.*, 2020, **142**, 18741-18745.
4. W. Liang, S. Zhu, K. Sun, J. Hai, Y. Cui, C. Gao, W. Li, Z. Wu, G. Zhang and H. Hu, *Adv. Funct. Mater.*, 2024, DOI: 10.1002/adfm.202415499.
5. D. Li, H. Zhang, X. Cui, Y. N. Chen, N. Wei, G. Ran, H. Lu, S. Chen, W. Zhang, C. Li, Y. Liu, Y. Liu and Z. Bo, *Adv. Mater.*, 2023, **36**, 2310362.
6. X. Liu, Y. Wei, X. Zhang, L. Qin, Z. Wei and H. Huang, *Sci. China Chem.*, 2020, **64**, 228-231.
7. L. Ma, S. Zhang, J. Zhu, J. Wang, J. Ren, J. Zhang and J. Hou, *Nat. Commun.*, 2021, **12**, 5093.
8. K. C. Song, B. J. Kim, W. Sung, S. G. Han, S. Chung, J. Lee and K. Cho, *J. Mater. Chem. C*, 2023, **11**, 5354-5362.

9. N. Yang, T. Zhang, S. Wang, C. An, S. Seibt, G. Wang, J. Wang, Y. Yang, W. Wang, Y. Xiao, H. Yao, S. Zhang, W. Ma and J. Hou, *Small Methods*, 2023, **8**, 2300036.

10. Z.-P. Yu, Z.-X. Liu, F.-X. Chen, R. Qin, T.-K. Lau, J.-L. Yin, X. Kong, X. Lu, M. Shi, C.-Z. Li and H. Chen, *Nat. Commun.*, 2019, **10**, 2152.

11. Y. Zhou, M. Li, H. Lu, H. Jin, X. Wang, Y. Zhang, S. Shen, Z. Ma, J. Song and Z. Bo, *Adv. Funct. Mater.*, 2021, **31**, 2101742.

12. D.-C. Lee, B. Cao, K. Jang and P. M. Forster, *J. Mater. Chem.*, 2010, **20**, 867-873.